



June 1992
Vol. 56, No. 1

U.S. Department
of Transportation
Federal Highway
Administration

Public Roads

A Journal of Highway Research and Development



Public Roads

A Journal of Highway Research and Development



June 1992
Vol. 56, No. 1

Cover art is a graphic illustration of highway signs. For exact specifications, please refer to the Manual on Uniform Traffic Control Devices.

U.S. Department of Transportation
Andrew H. Card, Jr., *Secretary*

Federal Highway Administration
Thomas D. Larson, *Administrator*

Office of Research and Development
Robert J. Betsold, *Acting Associate Administrator*

Editor
Anne N. Barsanti

Advisory Board
R.J. Betsold, T.J. Pasko, G.M. Shrieves,
and D.A. Bernard

NOTICE

The United States Government does not endorse products or manufacturers. Trade or manufacturers' names appear herein solely because they are considered essential to the object of an article.

Public Roads, A Journal of Highway Research and Development (ISSN 0033-3735; USPS 516-690) is published quarterly by the Office of Research and Development, Federal Highway Administration (FHWA), 400 Seventh Street SW, Washington, DC 20590. Second class postage paid at Washington, DC and additional mailing offices.

POSTMASTER: Send address changes to *Public Roads, A Journal of Highway Research and Development*, HRD-10, FHWA, 6300 Georgetown Pike, McLean, VA 22101-2296.

IN THIS ISSUE

Articles

- Developing a Standard Approach for Testing New Traffic Control Signs**
by Paul A. Pisano 1
- In-Vehicle Navigational Devices: Effects on the Safety of Driver Performance**
by Jonathan Walker, Elizabeth Alicandri,
Catherine Sedney and King Roberts 9
- Rock Riprap for Protection of Bridge Abutments Located at the Flood Plain**
by Jorge E. Pagán-Ortiz 23
- The FHWA Test Road: Construction and Instrumentation**
by Kevin Black and William Kenis 32

Departments

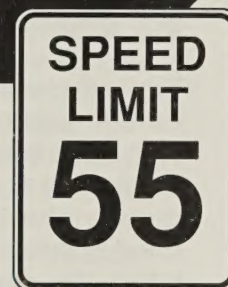
- Recent Publications** 40
- Technology Applications** 44
- New Research** 47

Public Roads, A Journal of Highway Research and Development, is sold by the Superintendent of Documents, U.S. Government Printing Office, Washington, DC 20402, for \$6 per year (\$1.50 additional for foreign mailing) or \$2 per single copy (50 cents additional for foreign mailing). Check or money order should be made payable and sent directly to New Orders Superintendent of Documents, P.O. Box 371954, Pittsburgh, PA 15250-7954. Subscriptions are available for 1-year periods.

The Secretary of Transportation has determined that the publication of this periodical is necessary in the transaction of the public business required by law of this Department.

Contents of this publication may be reprinted. Mention of source is requested.

DEVELOPING A STANDARD APPROACH FOR TESTING NEW TRAFFIC CONTROL SIGNS



by Paul A. Pisano

Introduction

Each year, the Federal Highway Administration (FHWA) receives requests to test and develop highway signs. Until now, these signs were tested by the Office of Safety and Traffic Operations Research & Development using whatever means seemed most appropriate at the time. Sign testing was often incorporated into other ongoing studies; thus, the sign testing methods used have varied over the years. Moreover, the subjects participating in these tests have been volunteers drawn from a master list maintained at the Turner-Fairbank Highway Research Center (TFHRC).

While this lack of standardization has been acceptable, it may not be the most effective or efficient way to do the work. First, the lack of consistency may well be reflected in the selection of functional signs; also, since the TFHRC subjects are not selected in a random manner, it is unclear if they represent a true sample of the driving public. Alongside these issues of the validity of the results is the fact that the lack of a prescribed method does not result in an efficient use of time or equipment.

To address these concerns, a study was recently conducted to:

- Develop a standard sign testing methodology.

- Identify which pieces of equipment should become standard for sign testing.
- Examine the possible self-selection bias in the TFHRC subject pool.

It is anticipated that the results of this study can be applied to other agencies that conduct sign tests on an irregular basis. In particular, the conclusions about the testing methodology can help other agencies manage the task of sign testing.

This article summarizes the study results, including recommendations about a standard sign testing methodology and comments on the validity of the TFHRC subject pool.

Developing a Standard Sign Testing Methodology

Two principal steps were involved in developing this methodology:

1. Determining the dependent variables to be tested.
2. Identifying the critical design criteria.

Dependent variables

The purpose of sign testing is to determine how well a candidate sign meets its prescribed func-

tion. Functionality is evaluated in terms of a sign's performance with respect to one or more measures of effectiveness (MOE's).

Over the years, many MOE's—including conspicuity, legibility, certainty of meaning, and comprehension—have been employed in sign testing. However, researchers have long debated as to which measures most effectively lead to a successful sign evaluation.

A 1985 study, upon reviewing the results of many previous studies, concluded that conspicuity and comprehension are the most important measures with respect to sign design. Conspicuity is a measure of how well a sign is noticed on the roadway. Comprehension is a measure of how well the sign's meaning is communicated. (1)¹

While these measures are important, there is one other measure to consider. Once the contents of a sign have been identified, drivers do not have to be looking at that sign to comprehend it. Consequently, the ease with which the contents are identified becomes just as important as the ease with which the sign is comprehended. This measure is known as recognition; and it differs from comprehension in that a sign does not have to be understood to be recognizable. (2)

Consequently, it was determined that these three MOE's—conspicuity, comprehension, and recognition—are critical to the success of almost every sign, and should be incorporated into a standardized sign testing system. Operational definitions for each measure were established based on a review of the literature, and previous studies conducted by the FHWA.

Conspicuity. As noted, conspicuity is a measure of how well a sign is noticed on the roadway. The more conspicuous a sign is, or the easier it is to spot with respect to other visual stimuli, the better it will serve its function. However, conspicuity can be very difficult to measure, since there are a myriad of situations that exist on the roadway. The success of this MOE is critically dependent on environmental attributes; there is no laboratory-based method that can be simply designed and implemented to measure this variable. Consequently, conspicuity was not included in the final version of the testing methodology.

Comprehension. Comprehension is a measure of how well the sign's meaning is communicated to the driver, as it relates to the function it is to serve. A straightforward way to measure comprehension is to assess the correctness of a subject's response—that is, compare the meaning that a

subject associates with a sign to that intended by the FHWA. If these meanings match, a sign can be considered to be understood. A sign can also be considered to be understood if a subject knows what response to take as a driver.

Recognition. Recognition relates to the identification of a sign's contents. For signs containing only text, this measure is commonly known as legibility. Generally, the easier it is to identify a sign's contents, the better the sign. For this measure, a subject does not need to comprehend the sign, just recognize its contents. There are several dependent variables that can be used to measure recognition. Two frequently used variables are response time and recognition distance. Response time measures the amount of time it takes for a subject to identify a sign's contents. Recognition distance measures the distance at which a sign's contents can be identified.

Design criteria

Data collection system. Once it was determined which dependent variables were to be measured, the next step was to determine how data collection was to take place. Certainly it would be economical to use a system that already existed, rather than build a new one. However, there were no such systems in place that would be available upon short notice. Therefore, it was necessary to design a new system that would be:

- *Compact*—since the system, when idle, could not occupy valuable work space at the TFHRC.
- *Portable and easy to manage*—since the equipment would possibly have to be assembled and dismantled every day at alternate data collection locations.

Given these system limitations, the dependent variables had to be easy to collect. As mentioned earlier, there did not appear to be any means of easily measuring conspicuity within the limits of a simple system. Comprehension, however, could be measured through the correctness of a subject's response. A sign could be displayed to the subject, who would then provide a response. The response would be evaluated based on its correctness.

Recognition could be measured either through response time or recognition distance. One way to collect response time data is to start a timer while displaying a sign to a subject. Once the subject identifies the sign's contents, he or she presses a button to stop the timer. The subject then verbalizes his or her interpretations to ensure that the contents were recognized; the response time is also recorded.

¹Italic numbers in parentheses identify references on page 8.

Data collection apparatus. The next step in the design process was to review data collection apparatuses used in previous studies. While it was expected that other configurations collected data for a different set of dependent variables, it was also expected that they could be modified to collect data for use in this study. From this review, the most promising apparatus clearly was that which was used in a 1988 FHWA study on seat belt signs. For this study, response time data were collected through the use of a Kodak Ektagraphic slide projector with an added shutter, a timer, and controls to operate the timer and the shutter. These pieces of equipment, along with a small rear-projection screen and all associated equipment, were contained on a 0.6-m by 0.9-m (2-ft by 3-ft) cart. (3)

This apparatus could easily be used to collect the data for the present study, since both comprehension and recognition data could be collected by showing slides onto the rear-projection screen. A shutter and timer were added to the configuration to collect the response time data. Other features were added to the setup to improve the experimental design and ease data collection. These features included adding a second slide projector to display a fixation point on which the subject could focus. A laptop computer with a detachable shelf was also added to reduce the time needed to

record subjects' responses. The final testing configuration is shown in figure 1.

Test protocol. Once the subject was selected, he or she was seated in front of the screen and handed the subject response button. The testing procedure was explained, and the subject was given the opportunity to ask questions. Response time data were collected first, and then comprehension data; this was because collecting the response time data shortly after the subject had just seen the same sign could have provided inaccurate data. However, this would not have been an issue if a sign was not tested for both comprehension and recognition for any one subject.

The experimenter sat by the side of the cart during the testing procedure, and the subject sat 1.4 m (4.5 ft) away from the cart, facing the screen that was attached to it. At this distance, and given the size of the image on the screen, this was equivalent to viewing a sign in the field at a distance of 30.5 m (100 ft). Once the introduction was completed, the experimenter ran the subject through three test signs to ensure that the directions were understood. Before displaying each sign, the experimenter would say, "next," which would act as a signal to mentally prepare the subject for the next slide (the sub-

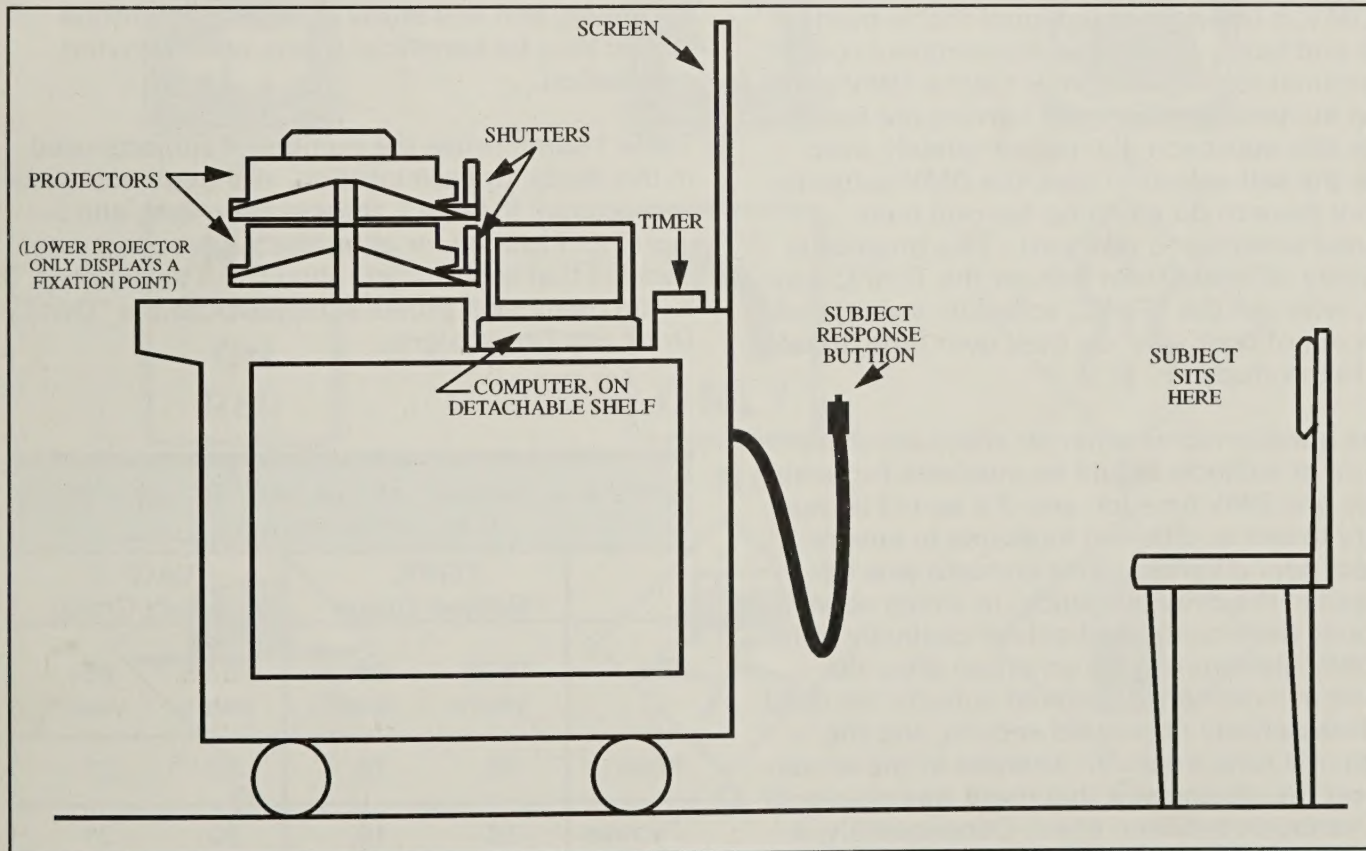


Figure 1.— Final testing configuration.

ject would already be visually prepared since he or she was focused on the fixed point).

Test Subjects

The sample of test subjects must be representative of the general population in order for study results to be valid. Because the TFHRC subjects are self-selected, volunteering to participate in given studies, it is not known if they represent a true sample. To determine if the TFHRC subject pool is a valid sample, these subjects were compared to another, non-self-selected set of participants. If no significant difference was found between the two pools, it would be acceptable to continue using the TFHRC subject pool.

The first task in studying the TFHRC subject pool was to find an adequate comparison group that:

- Was not self-selected.
- Represented a good cross section of the driving public (i.e., contained people of varying ages, both sexes, and different races, cultures, and socioeconomic backgrounds.)
- Consisted of licensed drivers.

It was determined from a previous study that the Department of Motor Vehicles (DMV) could provide this pool. (4) Since all licensed drivers use the DMV, it offers a subject pool that is both large and easily accessible. Researchers could set up their testing equipment at the DMV and select subjects as they were leaving the facility. While this approach did not completely overcome the self-selection bias, the DMV subjects did not have to do anything beyond their planned activities to take part. This process is distinctly different from that for the TFHRC subjects, who call the TFHRC, schedule a visit, and drive out of their way, on their own time, to take part in the study.

It was questioned whether an adequate cross section of subjects would be available for testing at any one DMV location and if it would be necessary to test at different locations to ensure subject pool diversity. This concern was addressed in the previous study, in which screening tests were conducted at four distinctly different DMV stations (one in an urban area, the second in a densely populated suburb, the third in a less densely populated suburb, and the fourth in a rural area). (4) Analysis of the screening test results showed that there was no significant variation between sites. Consequently, it was determined that a local office of the Virginia DMV would provide the needed comparison

pool for the present study. This site was chosen for its convenience to the TFHRC, in case study results indicated that future sign testing would need to be conducted at the DMV.

For this study, recognition data were collected on 18 signs, and comprehension data were collected on 15. The set of test signs included some taken directly from the *Manual on Uniform Traffic Control Devices (MUTCD)*, as well as new signs that the subjects had never seen before. These new signs included variations on standard signs, samples of a seat belt sign, and a "Don't Drink and Drive" sign, among others. The three signs that were tested only for recognition were not included in the comprehension tests because they depicted a symbol that was not expected to convey any specific meaning with respect to the driving task. Figure 2 shows all 18 signs.

The recognition data were collected for each sign, and then the comprehension data were collected. The subjects tested at the TFHRC were between the ages of 18 and 25 and those over 65. This gap in ages was because they were taking part in another study that focused on older and younger drivers. The subjects tested at the DMV were of all ages; data were used, however, only for those age groups corresponding to the TFHRC sample. The age composition of the subjects was justified by the fact that drivers at these ages are overrepresented in accidents, and any study of these age groups would thus be beneficial to the whole driving population.

Table 1 summarizes the number of subjects used in this study for each location. Although not taken into account in table 1, three signs—G, H, and I—were not included for all subjects, because it was decided that each subject should not be exposed to too many high profile signs, such as the "Don't Drink and Drive" signs.

Table 1.—Number of subjects in each group by sex and age

	TFHRC Subject Group		DMV Subject Group	
	18-25 years	65+ years	18-25 years	65+ years
Sex				
Male	10	10	30	27
Female	10	10	30	21

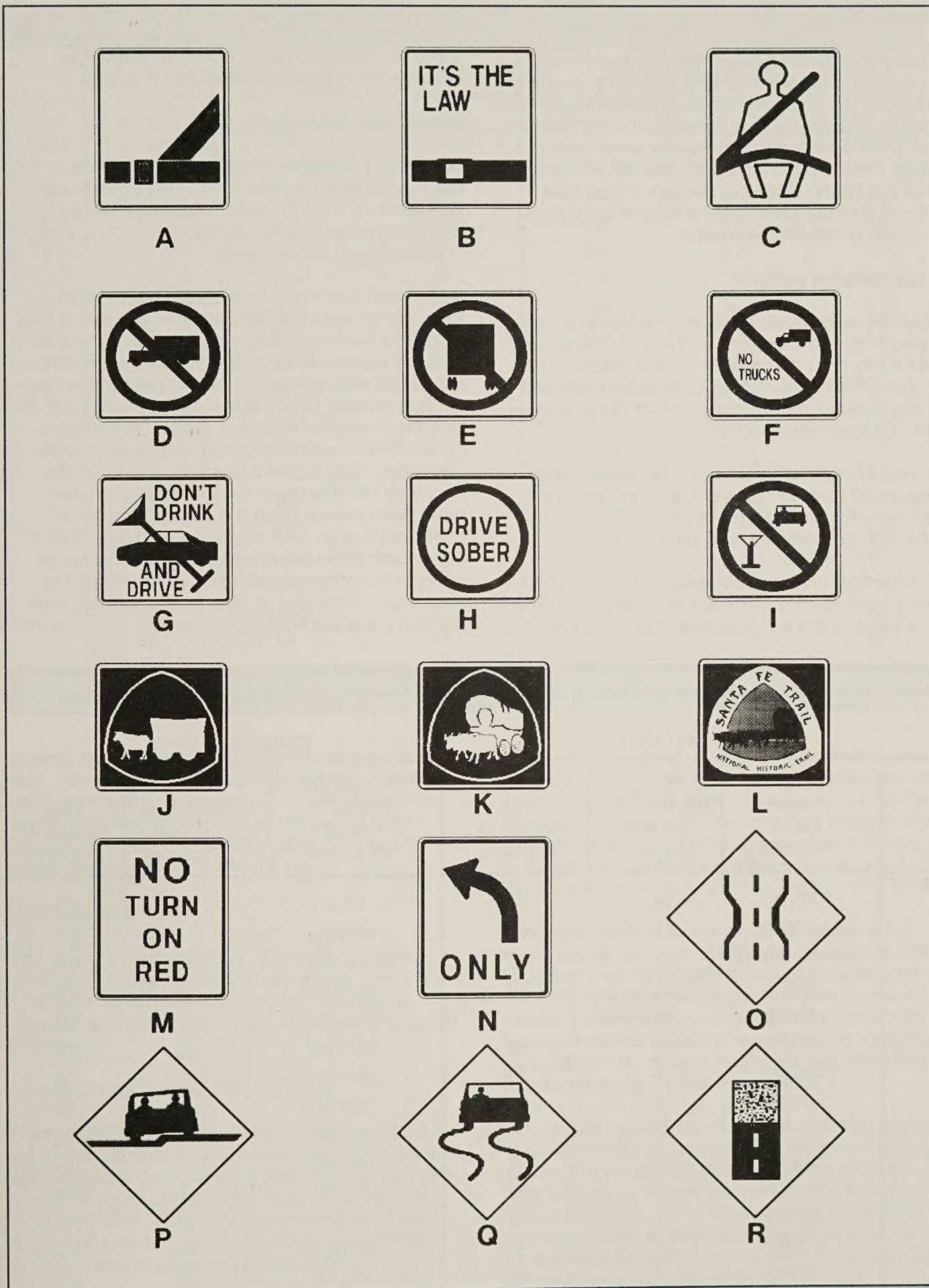


Figure 2.—Signs included in the study.

Results

In summary, the MOE's selected for the standard sign testing methodology and used as a means of evaluating the signs were comprehension and recognition. The respective dependent variables for these MOE's were response correctness and response time. Comprehension was the primary focus of the study, since it is the most important MOE. The study's statistical analyses were computed using SYSTAT software.

Comprehension analysis

Response correctness data were collected by displaying a sign to a subject, and having the subject voice his or her interpretation of the meaning of the sign. The experimenter then either recorded the correctness of the response, or the response itself, if it was noteworthy.

The responses were compiled, reviewed, and categorized to determine correct and incorrect responses for each of the 15 signs. The results of this categorization are in table 2.

Once the correctness data were categorized, Chi-square tests were conducted to determine if the percentage of correct responses between the

two subject groups was the same. The results of the Chi-square test revealed that, at the 0.05 level, there was no significant difference between subject groups for any of the signs.

Response time analysis

Before any analyses could be conducted on the response time data, each data record was reviewed. If a record was unacceptable (e.g., no response was given by the subject), it was dropped from the analysis.

Next, tests were run on the acceptable data. First, summary statistics, such as the mean and standard deviation, were computed. These statistics are provided in table 3. Following this, each sign was analyzed with respect to the two subject groups to see if there was significant difference between response times. The Kolmogorov-Smirnov test was conducted, with comparisons made at the 0.05 level. This test determines whether two independent samples have been drawn from the same population. It would thus show if there were a statistically significant difference between the percentage of correct responses for the two locations for each sign. (SYSTAT is able to account for differing sample sizes when running this test—an im-

Table 2.—Summary of responses of the comprehension data

Sign	TFHRC Subject Group			DMV Subject Group		
	Number and Percent of Correct Responses	Number of Incorrect Responses	Total Number of Responses	Number and Percent of Correct Responses	Number of Incorrect Responses	Total Number of Responses
A	30 (75)	10	40	87 (81)	21	108
B	37 (92)	3	40	104 (96)	4	108
C	32 (80)	8	40	90 (83)	18	108
D	38 (95)	2	40	102 (94)	6	108
E	32 (80)	8	40	76 (70)	32	108
F	37 (92)	3	40	106 (98)	2	108
G	20 (100)	0	20	56 (100)	0	56
H	39 (98)	1	40	55 (98)	1	56
I	38 (95)	2	40	49 (88)	7	56
M	40 (100)	0	40	107 (99)	1	108
N	40 (100)	0	40	108 (100)	0	108
O	34 (85)	6	40	88 (81)	20	108
P	25 (62)	15	40	72 (67)	36	108
Q	32 (80)	8	40	82 (76)	26	108
R	18 (45)	22	40	52 (48)	56	108

Table 3.—Summary statistics of the recognition data

Sign	TFHRC Subject Group			DMV Subject Group		
	Sample Size	Response Time		Sample Size	Response Time	
		Mean	Deviation		Mean	Deviation
A	39	2.55	2.57	104	2.59	2.52
B	39	2.49	1.49	106	1.96	1.03
C	40	3.07	2.78	106	2.60	2.24
D	40	1.42	0.99	106	1.55	1.08
E	40	2.72	2.00	105	3.12	2.15
F	40	2.42	1.79	104	1.92	1.11
G	20	3.22	2.24	55	2.06	1.26
H	40	1.62	0.93	55	1.55	0.88
I	40	2.70	2.14	48	2.11	1.17
J	39	2.60	2.27	106	2.55	1.83
K	39	2.57	1.92	104	2.66	1.79
L	38	4.59	3.47	100	4.45	3.47
M	40	1.15	0.56	103	1.46	1.06
N	40	1.39	0.78	108	1.59	1.03
O	39	2.26	1.66	106	2.61	2.24
P	39	2.48	2.56	107	2.82	2.64
Q	40	1.87	1.34	107	1.90	1.67
R	39	4.80	3.39	104	4.45	3.30

portant consideration when performing the K-S test.) Cumulative distributions were plotted for each sign, providing a graphic comparison between the response times of the two subject groups. No significant difference was found in the responses of the two groups.

Discussion

The study's methodology, although successful in achieving the present study goals, could be improved to enhance the research findings. Specific methodological concerns are discussed below.

Standard sign testing methodology

The most prominent concern with the methodology involved collecting the response time data. It was apparent that a few subjects tried to comprehend the sign, rather than simply identify each sign's contents. The most effective way to address this problem would be to improve the instruction and training of the subjects.

A second concern relates to the recognition MOE. The existing procedure was able to account for

the temporal aspects of recognition, that is, the amount of time it takes to recognize the sign; however, it did not incorporate the distance aspects. While measuring only the temporal aspects is acceptable as a means of measuring recognition, it may also be worthwhile to measure recognition distance in order to more fully explore this MOE.

The third drawback of the methodology is the static nature of the presentation. Using the FHWA Highway Driving Simulator could provide a dynamic testing methodology; however, it would first be beneficial to compare results from both testing methodologies to see if there is a significant difference. It may be shown that the static methodology is, in fact, acceptable.

Finally, the system could be improved by adding some measure of conspicuity. As discussed above, it was not feasible to recreate all of the different roadway scenarios to measure fully this MOE. However, some sign-specific dependent variables, such as color preference or ratio of background to legend, could be included to measure some conspicuity aspects.

Testing equipment

The testing equipment used in this study performed well. Using the Ektagraphic slide projector with an added shutter to control viewing onto the rear-projection screen proved to be an effective means of collecting comprehension data. Also, having the added timer—which measured the amount of time the shutter was open—proved successful for collecting the recognition data. Other features of the setup, including the small mobile cart and the laptop computer, also performed well, with no flaws identified.

With this setup, the response time on the timer was manually entered into the laptop. This configuration worked well, and was found to be time-efficient. However, it may be worthwhile to link the timer with the laptop to enable response time to be automatically downloaded. Such a configuration would save time and eliminate the potential for transcription errors.

Test subjects

The only concern regarding test subjects had to do with the fact that the test was still voluntary at the DMV. This element of choice meant that drivers with the poorest abilities could still decline to participate in the study. Therefore, the DMV subjects were not a true cross section of the driving public. However, the self-selection bias was much weaker with the DMV subject group than with the TFHRC group; moreover, the composition of this group was significantly different from the TFHRC subject group.

Conclusion

The three goals of this study were successfully met, although the study's methodology could be enhanced, as discussed above. Specifically, an efficient and consistent testing methodology was developed, using equipment that was compact, portable, and easy to manage. Furthermore, by comparing the TFHRC subjects to a distinctly dif-

ferent subject pool, it was determined that the difference between these two pools was not statistically significant. Consequently, the potential bias found in the TFHRC subjects does not affect the outcome of FHWA studies that use these subjects.

The results of this study will be helpful for agencies that conduct sign tests on an irregular basis. The methodology developed is very straightforward, and most of the equipment is available off the shelf. Also, implementing such a system should not be time- or cost-intensive. Since the timer and response button would probably have to be assembled, the system enhancement linking the timer and laptop directly would be incorporated at the time of that assembly. The only other aspect of the methodology that may require outside assistance is the development of the stimulus slides. However, some graphic software companies provide such slide preparation services.

References

- (1) M.T. Peitruca and R.L. Knoblauch. *Motorists' Comprehension of Regulatory, Warning, and Symbol Signs, Volume I: Executive Summary*, Biotechnology, Inc., Falls Church, VA, 1985.
- (2) R.E. Dewar and J.G. Ells. "Methods of Evaluation of Traffic Signs." *Information Design: The Design and Evaluation of Signs and Printed Material*, Ronald Easterby and Harm Zwaga, eds., New York: John Wiley and Sons Ltd., New York, 1978, pp. 77-90.
- (3) E. Alicandri and K. Roberts. "An Evaluation of Symbols for a Regulatory Seat Belt Sign." unpublished internal report, Turner-Fairbank Highway Research Center, 1988.
- (4) M.T. Peitruca and R.L. Knoblauch. *Motorists' Comprehension of Regulatory, Warning, and Symbol Signs, Volume II: Technical Report*, Biotechnology, Inc., Falls Church, VA, 1985.

Paul A. Pisano is a highway research engineer in the Office of Safety and Traffic Operations R&D, Information and Behavioral Systems Division, Federal Highway Administration.

In-Vehicle Navigational Devices:

Effects on the Safety of Driver Performance

by Jonathan Walker, Elizabeth Alicandri,
Catherine Sedney, and King Roberts

Introduction

Although an onboard navigational device may aid drivers in a given task, its operation may also introduce significant hazards. For example, when investigating cellular telephone use, it was estimated that almost 12 percent of drivers would go out of their lane while placing a call. (1)¹

Onboard systems compete with other elements of the driving task for the user's attention. Consequently, use of a guidance device may impose additional demands that could offset the benefits of assisted navigation.

Among the most basic of system design issues is the quantity and type of guidance information that should be provided, and the method by which it should be presented. This article presents the findings of a recent Federal Highway Administration (FHWA) study that examined these and related issues. The study was based on the assumptions that (1) use of any onboard device adds to the demands of the driving task and (2) at some level of increase, use of the device may cause an unacceptable deterioration in

driving safety. The study's purpose was to gauge the safety of drivers' performance when using guidance devices of varying complexity and mode of presentation.

Method

Subjects

Licensed drivers were either drawn from the subject listing maintained by the Turner-Fairbank Highway Research Center (TFHRC) or recruited from the greater Washington, D.C. metropolitan area. The sample consisted of 126 subjects, in three age ranges:

- Younger, 20 to 25, average age of 22.8 years.
- Middle, 35 to 40, average age of 37.6 years.
- Older, 55 and older, average age of 62.8 years.

This sample allowed for 18 subjects in each of the 7 experimental conditions. Subjects were also balanced by gender.

¹Italic numbers in parentheses identify references on pages 21-22.

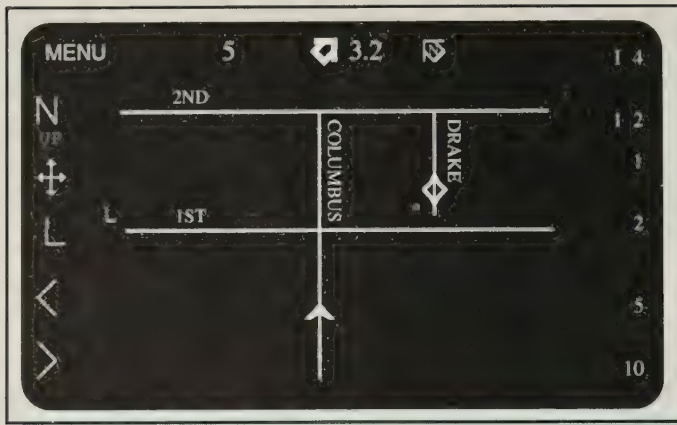


Figure 1.—Sketch of complex visual guidance unit display.

Apparatus

Simulator. Data were collected as subjects drove in the FHWA's Highway Simulator (HYSIM). The HYSIM is a fully interactive driving simulator using computer-generated graphics for roadway delineation. A more complete description of the HYSIM is in appendix A of the study's final report. (2)

Guidance units. Six electronic guidance units—three visual and three audio—were used. The complex visual unit consisted of a screen showing a map of the area in the driver's immediate vicinity (figure 1). The unit represented the driver and the destination as icons on the map; the map "flowed" as the driver proceeded through the road system.

Figure 2 illustrates the medium complexity visual unit, which was a modification of the Electronic Route Guidance System (ERGS). (3) An example of its operation would be if the driver was to make a left turn, the system would light up "TAKE THIRD LEFT" in the third block before the turn, "TAKE SECOND LEFT" in the second block, etc.

The simple visual unit was also a modification of ERGS; it used only the turn arrows on the ERGS display, lighting the appropriate arrow just before the driver was to make a turn (figure 3).



Figure 2.—Sketch of medium visual guidance unit display.

The audio guidance units were designed to parallel the visual systems. The complex audio system was a recorded series of statements, in a woman's voice, giving as much information as feasible regarding the driver's whereabouts. These messages occurred periodically along the drive. The text of these messages is in appendix B of the final report. (2)

The medium complexity audio unit presented a spoken version of the corresponding visual unit (e.g., "Take third left").

The simple audio system also corresponded to the visual system. The driver heard a female voice say "left, left, left" or "right, right, right" half a block before a turn.

Control condition. The seventh experimental condition, was a control designed to give the best navigational information without electronics. Subjects in this condition were given a "strip" map similar to those used by the American Automobile Association. The length of each strip covered only the previous and next turns, and included written directions. Every street and grade crossing between the two turns was on the map. Subjects turned to the next strip at the first stop sign after each turn. They were also permitted to look at the map at any other stop sign or red traffic light. Subjects could not look at the map while driving because of the dark car interior. A sample page of the map is in appendix C of the final report. (2)

Scenario

The scenario the subjects drove in the HYSIM was based on roads in Detroit, Michigan. Width and number of lanes were manipulated by the experimenters. Side streets that were not part of the route (i.e., wrong turns) ended in cul-de-sacs. This strategy not only brought the drivers back to the point at which they left the correct route, but also allowed for greater emphasis on

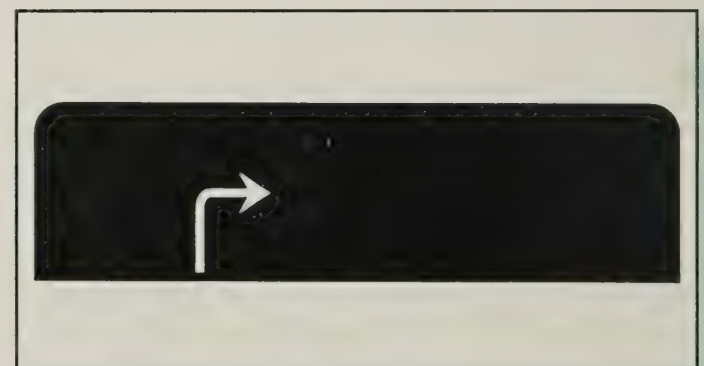


Figure 3.—Sketch of simple visual guidance unit display.

the effectiveness of the guidance units on driving performance as opposed to their effectiveness in aiding route-following.

Signs in the main drive were developed using guidelines for urban signing from the *Manual on Uniform Traffic Control Devices (MUTCD)*. (4) All streets within three blocks of a turn were signed—a necessity for drivers in the map control group. Other signs included standard regulatory, warning, and guide signs. The speed limit was 40 km/h (25 mi/h) throughout the drive, with a physical cap on the simulator car of 48 km/h (30 mi/h).

Loading

Three types of loading (psychomotor, perceptual, and cognitive) were changed during the main drive to increase the workload of the driving task. The first third of the drive had the lowest loading (“easy”), the second third of the drive had “moderate” loading, and the last third had the most loading (“hard”). The loading tasks are detailed below, and charted in table 1.

Psychomotor. Three factors were involved in the psychomotor loading: lane width, intensity of crosswinds, and presence of another vehicle.

In the easy section, the subject drove on two-lane streets with 4-m (12-ft) lanes. There were no crosswinds and no other vehicle was present, thereby providing a “best case” scenario.

In the medium section, the subject drove on a four-lane street with lanes narrowed to 3 m (10 ft). Some light crosswinds were present, and an other

vehicle, located in the adjacent lane, “tracked” the subject throughout this section of the drive. The speed of the car was matched to the subject’s speed with slight variations. The car never prevented the subject from turning, and dropped out of sight before turns and at other points in the scenario.

In the hard section of the drive, the lanes were 2 m (8 ft) wide. The crosswinds increased in intensity, and the other vehicle was a 10-wheel dump truck which tracked the subject in the manner described above.

Perceptual. The perceptual loading involved monitoring two of the gauges on the dashboard: oil and temperature. The subject was told that if either gauge went out of normal range, it should be reset as quickly as possible by pushing the button above it.

In the easy section of the drive, both gauges remained in the midline state. In the moderate section of the drive, one of the gauges changed from fully in to fully out. In the hard section, one gauge changed from barely in to fully out. This latter difference was much more difficult to perceive than the full change in the medium section.

Cognitive. The cognitive loading task consisted of a tape-recorded series of mental arithmetic problems. The calculations involved a combination of distance to the next gas station and remaining fuel. They varied in difficulty depending on the drive section. The mileage problems used are in appendix D of the final report. (2)

Table 1.—Factors used to increase driving task load

Load Factor	Section of Drive		
	Easy	Moderate	Hard
Lane Width	12ft.	10 ft.	8 ft.
Cross winds	None	Light	Heavy
Other Vehicle	None	Sedan	Truck
Gauge Change	None	Gross	Small
Mileage Questions	Easy	Moderate	Hard

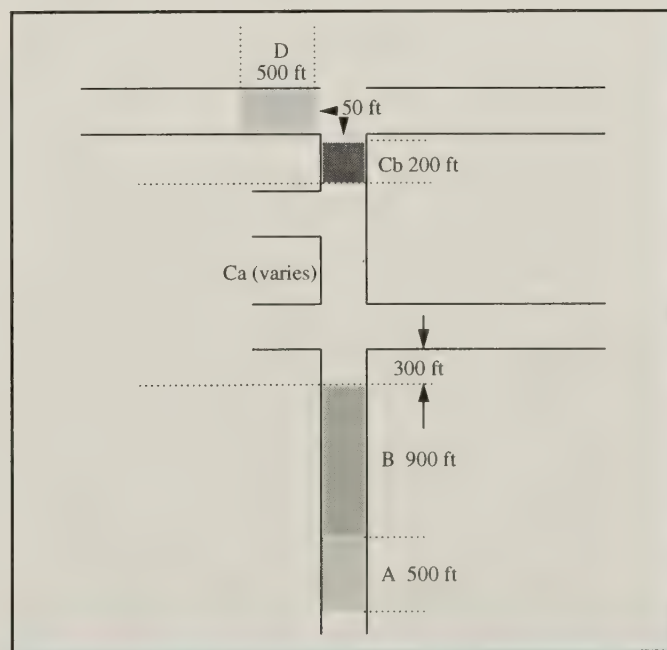


Figure 4.—Definition of subzones in zones which included a turn.

Data zones

There were 15 data zones in the scenario, 5 in each third of the drive. Of these data zones, 12 included turns (4 in each third), and 3 were in straight segments of the drive (1 in each third). The straight zones were designed as control conditions that had no guidance information. The data zones which included turns were numbered from 1 through 12; the straight zones were designated by an alphabetic character: X (easy), Y (medium), and Z (hard).

Each data zone was divided into subzones: A, B, C, and D (figure 4). In the simple treatment, subzone C was further divided into Ca and Cb. The subzones were devised to detect driving behaviors attributable to different types of loading, and interactions—if any—of load and the various guidance devices.

Dependent variables

Data were collected in the simulator at a rate of once every .075 s, then averaged over each subzone. Four basic types of data were collected during the drive:

- *Heart rate*—each subject's resting heart rate, in beats per minute, was measured for use as a baseline; heart rate data were then collected in every subzone. Data were adjusted for individual differences to yield percentage change for each data point.
- *Reaction time*—reaction time to gauge changes was collected only once in each data zone of the medium and hard sections. Reaction time was defined as the time from the changing of the gauge to the subject's response of pressing the appropriate button.
- *Speed*—four speed variables, minimum, mean, variance, and skew, were recorded in each subzone.
- *Lateral placement*—lateral placement data were collected in every subzone. The center of the "correct" lane (the lane in which the driver should have been) was given the value of 0; deviations were measured based on placement of the center of the HYSIM car relative to the zero point. Deviations in the direction of the next turn or away from the simulated "other vehicle" were counted as positive; other deviations were counted as negative. The raw lateral placement data were converted to ratios to equalize the scores. All data points were divided by the leeway—i.e., the distance from the side of the car to the edge of the lane when the car was centered in its lane. Leeway changed in each drive section. Data over +1 indicated that the car was out of its lane.

Procedure

Upon arriving at the research center, each subject took a vision test and had his/her pulse taken to establish a baseline for heart rate data.

Next, the experimenter described the HYSIM car controls, read the study instructions to the subject (appendix F in the final report), and gave the subject an overview map of the practice route. (2) Subjects in the complex visual condition were shown a simplified map similar to the visual display; subjects in the control group were given strip maps of the practice route.

The experimenter then demonstrated the driving characteristics of the system. After a demonstration of two turn maneuvers, the subject took the driver's position. The plethysmograph was attached to monitor heart rate, and the subject was allowed a practice session that encompassed use of the guidance system, vehicle operation, and posing of cognitive questions. Subjects were encouraged to continue the session until fully comfortable with the vehicle and procedures.

The subject was given a brief break while the main drive was loaded into the HYSIM computer. At this time subjects in the control group were given strip maps for the main drive.

During the drive, the experimenter monitored the subject's progress from the control room adjoining the HYSIM laboratory. If any error was made in following the route, the experimenter verbally guided the subject out of the cul-de-sac and back onto the appropriate path. In the event of a crash, an attempt was made to restart the drive at the point of the crash. In a small number of cases, the program was reloaded, and the experimenter drove the car back to the point of the crash.

Results

Heart rate

Analysis of the heart rate data found no device effects and no age effects, although there was a significant interaction of loading and subzone ($F = 5.37$, $df = 6/462$, $p = 0.0001$). Heart rate was not responsive to overall loading sections, nor did it differentiate among the navigational devices.

Reaction time

Gauges changed only during the middle and final third of the drive. Thus, each subject had 10 trials, including the straight zones, for a total of 1,260 trials over the whole experiment. Of these, the subjects pressed the response button on 1,052 trials,

for a "hit" percentage of 84. Subjects missed 201 trials, for a "miss" percentage of 16. Seven trials were declared unknown because all the data for those zones were missing, generally due to subjects crashing or suffering from simulator sickness. The miss percentage was much larger than expected, resulting in a loss of 28 subjects in the analysis of variance.

No sex or loading effects were found in the analysis, but there were significant turn effects, with significant interactions between turn and device and between turn and age group.

The reaction times in turn zones averaged 6.79 s longer than those in straight zones ($F = 31.14$, $df = 1/84$, $p = 0.0001$). By treatment, differences were largest for the complex visual and map devices—20 and 10 s, respectively. All auditory devices and the simple visual device had a 2-s difference; the medium visual device had a difference of 6 s.

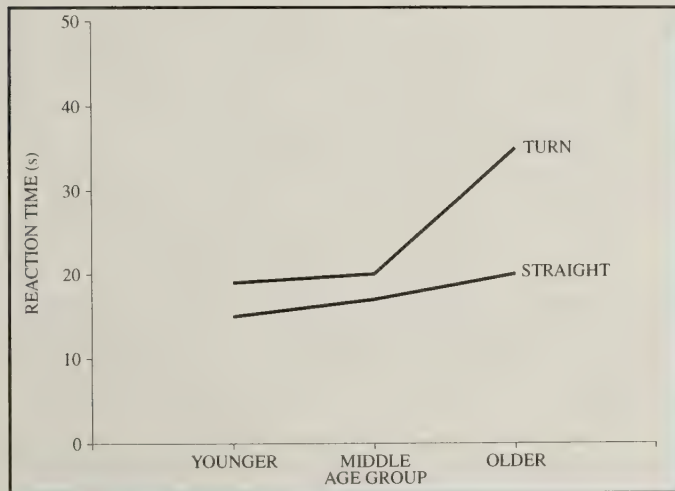


Figure 5.—Averages of reaction times to gauges, broken down by age, group, and type of zone.

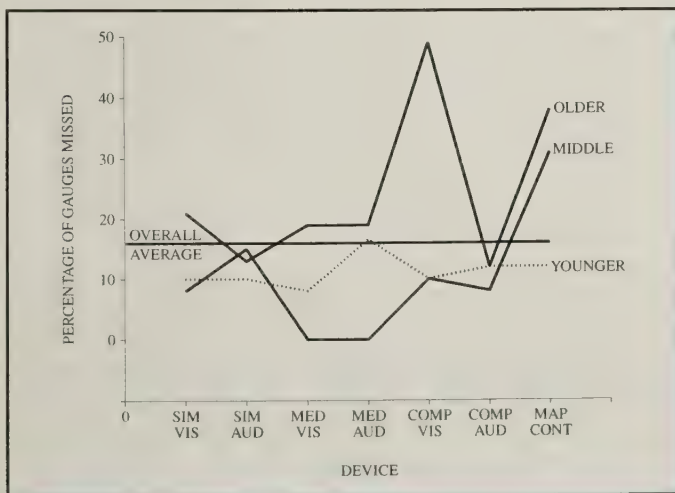


Figure 6.—Percentage of gauges missed, broken down by device and age.

A possible explanation for these differences lies in the subjects' use of street signs. In the map-control group, subjects could not make a turn without reading the signs; looking for street signs takes time away from looking at gauges. While this interpretation also seems reasonable for the complex visual group, it is more likely that for this group, time spent scanning the electronic map took time away from watching for gauge changes. Figure 5 shows the turn-by-age-group interaction ($F = 11.5$, $df = 2/84$, $p = 0.0001$). The overall turn effect is again evident, along with an age effect. This latter effect is linear except for the older subjects during turns, indicating that choice-points are particularly demanding for older drivers. This strong interaction emphasizes the need to include this group in driving studies.

Because there was a fairly large percentage of misses, a frequency analysis of hits versus misses was performed. The significant results follow those of the reaction time analysis with a few exceptions (figure 6).

- There were no overall effects for sex or loading.
- There was an overall age effect (Chi-square = 35.53, $df = 2$, $p = 0.000$), with the older subjects missing more than the other two groups.
- There was a significant interaction between age group and device (Cochran-Mantel-Haenszel chi-square = 37.26, $df = 2$, $p = 0.000$).

The analysis tested age group versus gauge-hit-or-missed for each device. The complex visual group had the largest differences (Chi-square = 30.16, $p = 0.000$), followed by the medium visual group (Chi-square = 12.49, $p = 0.002$), the medium audio group (Chi-square = 11.97, $p = 0.003$), and the map-control group (Chi-square = 11.93, $p = 0.003$). There were no significant age-group differences within the other three groups (simple visual, simple audio, and complex audio). The hit/miss pattern of the older subjects is similar to their reaction time pattern. On the other hand, the pattern of the middle-aged group is quite different. The middle-aged map control subjects missed almost as many gauges as the older subjects, but the middle-aged subjects who used the medium visual or medium audio devices missed none—significantly less than either the older or younger subjects using those devices.

Speed

Average speeds. As in the reaction time data, a turn factor was added to the analysis to compare the straight zones to the turn zones (figure 7). As expected, the straight zones showed relatively little change in speed, whereas in the turn zones

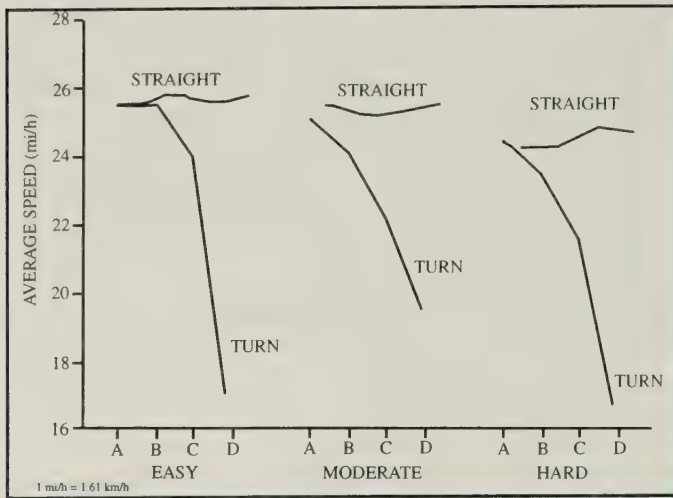


Figure 7.—Average speeds, broken down by turn, loading, and subzone.

the drivers slowed, especially before the turn (subzone C) and after the turn (subzone D). In the analysis of variance, this is shown in a significant turn effect ($F = 478.7$, $df = 1/83$, $p = 0.0001$), and a turn-by-subzone interaction effect ($F = 670.7$, $df = 3/249$, $p = 0.000$). Because this interaction was so large, separate analyses were computed for the turn zones and the straight zones.

There were no treatment, age, or sex differences in the analysis, either as main effects or as interactions with the within-subjects factors. It could have been expected that the groups using the simple and medium devices—which presented no navigational information during these zones—would have been faster than the map control or complex visual groups, which had information available, or the complex audio group, which heard a message within subzone C of the straight zones. If drivers in these three groups took in any navigational information, it did not affect their speeds, perhaps because they did not have to act upon it.

The *straight-zone* analysis did uncover a significant loading effect ($F = 12.49$, $df = 2/166$, $p = 0.0001$), a significant subzone effect ($F = 4.23$, $df = 3/249$, $p = 0.0061$), and a significant interaction of the two ($F = 4.34$, $df = 6/498$, $p = 0.0003$). Profile contrasts indicated that speeds in the hard loading section were 1.9 km/h (1.2 mi/h) slower than in the moderate section. This difference was significant ($p = 0.0002$), whereas the difference between the easy and moderate sections .32 km/h (.20 mi/h) was not ($p = 0.32$). Naturally, decreases in speed were expected as loading increased. Unfortunately, the techniques used did not give a linear function of speed to loading, as there was no significant decrease from the easy to the moderate section.

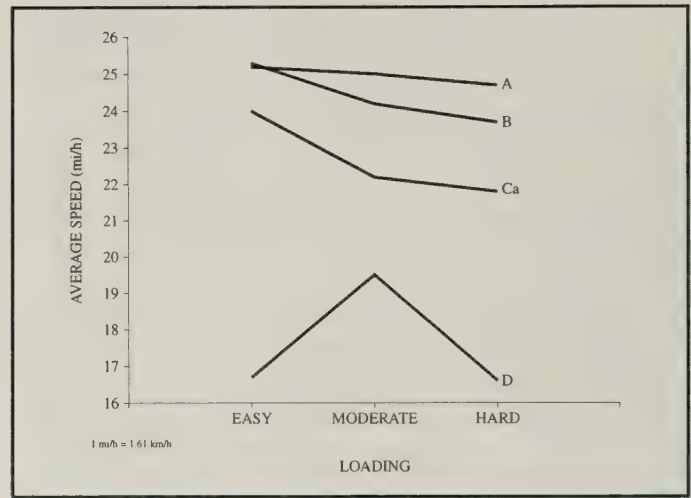


Figure 8.—Average speed around turns, broken down by loading and subzone.

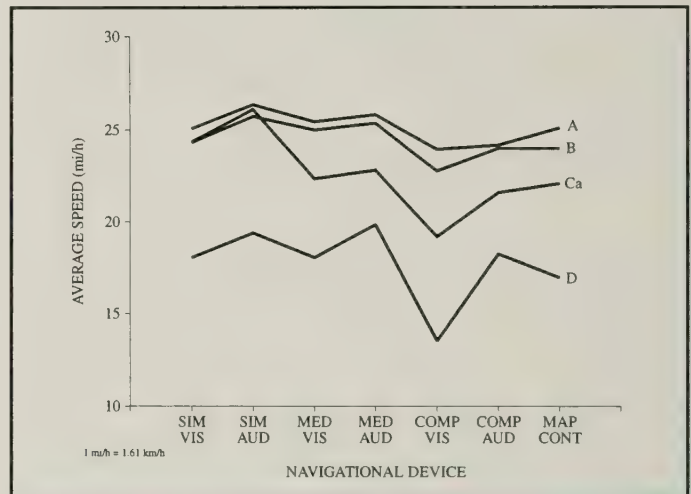


Figure 9.—Average speed broken down by subzone and treatment.

To investigate the other significant straight-zone effects, the speeds were broken down by loading and analyzed separately. These analyses showed that there was a significant difference within subzones only in the hard section ($F = 5.12$, $df = 3/252$, $p = 0.0019$), with an increase of 1.08 km/h (0.67 mi/h) between subzones B and C. The most plausible explanation is that the gas mileage problems heard at the beginning of subzone B were sufficiently difficult in the hard zone to slow the driver; however, this does not explain why average speeds in subzone A were just as slow as in subzone B.

In the analysis of the speed data for the turn zones by themselves (collapsed into an average for each loading section), the largest effect was for subzone ($F = 901.84$, $df = 3/252$, $p = 0.000$) (figure 7). Analysis also revealed an obvious loading effect ($F = 66.1$, $df = 2/168$, $p = 0.0001$), and a strong loading-by-subzone interaction ($F = 153.98$, $df = 6/504$, $p = 0.000$), which is mainly due to slower

than expected speed in subzone D of the easy loading section (figure 8). One possible explanation is that the turns on two-lane streets were much more difficult than turns on four-lane streets, even though the two-lane streets were .6 m (2 ft) wider per lane.² Another possible explanation is that right turns are harder than left turns; and because the moderate section had only one right turn, its speeds in subzone D were higher. To decide between these possibilities, the average speeds in all 12 zones were inspected. Left turns were no different than right turns, a result that favors the former explanation.

There was a significant overall navigational device effect ($F = 9.58$, $df = 6/84$, $p = 0.0001$). In addition, there were significant interactions with loading ($F = 3.28$, $df = 12/168$, $p = 0.0003$), subzone ($F = 10.24$, $df = 18/252$, $p = 0.0001$), and the combination of loading and subzone ($F = 2.05$, $df = 36/504$, $p = 0.0004$).

Figure 9 illustrates the overall treatment differences and the subzone-by-device interaction. In all subzones, the complex visual group had the slowest speeds with one exception—subzone A of the easy section. In subzone D, it was significantly slower than all of the other groups. In subzone A, it was significantly different from the simple audio group, but none of the others. In subzones B and C, the differences depended on the loading section.

There were no significant treatment differences in the easy section for subzone B ($F = 1.82$, $df = 6/84$, $p = 0.1056$) (figure 10). The range among groups was 3.4 km/h (2.1 mi/h). In the moderate section (figure 11) during subzone B, the complex visual group was significantly slower than the medium

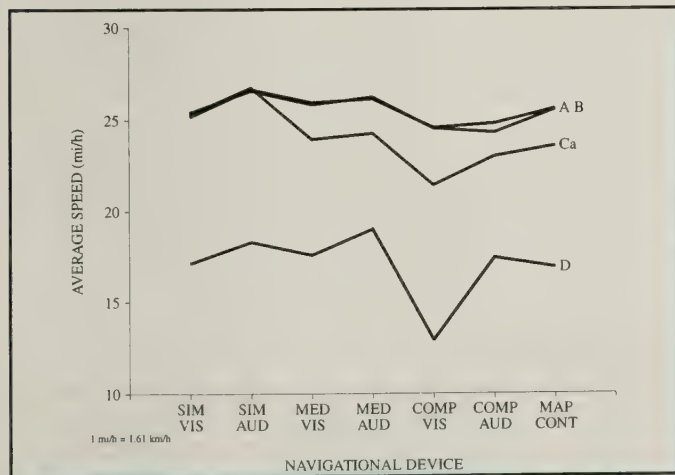


Figure 10.—Average speed broken down by treatment and subzone, easy loading only.

²This difficulty stems from certain limitation in the HYSIM graphics component which affect the appearance of intersections.

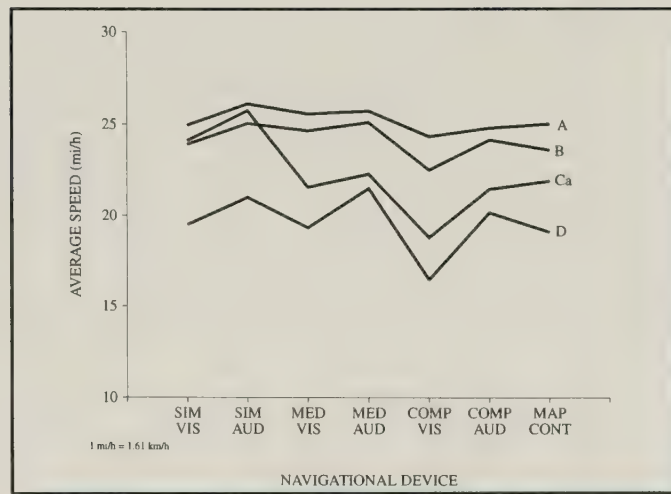


Figure 11.—Average speed broken down by treatment and subzone, moderate loading only.

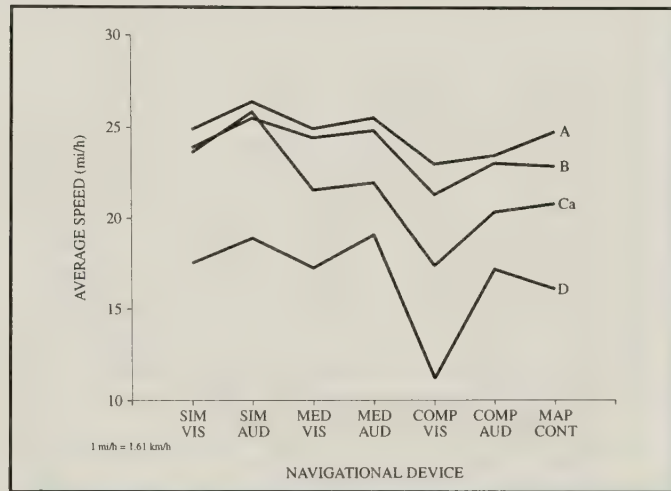


Figure 12.—Average speed broken down by treatment and subzone, hard loading only.

audio group. The difference here was 4.3 km/h (2.7 mi/h), which is a marginal difference as indicated by the overall treatment effect ($F = 2.38$, $df = 6/84$, $p = 0.0357$). In the hard section (figure 12), the complex visual group (34.3 km/h [21.3 mi/h]) is significantly slower than the simple audio (41.1 km/h [25.5 mi/h]), medium audio (39.9 km/h [24.8 mi/h]), and medium visual (39.3 km/h [24.4 mi/h]) groups ($F = 4.39$, $df = 6/84$, $p = 0.0007$).

For subzone C in the easy section (figure 10), the complex visual group (34.4 km/h [21.4 mi/h]) is slower than all other groups except the complex audio group (37.0 km/h [23.0 mi/h]) ($F = 11.1$, $df = 6/84$, $p = 0.0001$). Note that the complex visual is the only group slower than the map control group. In the moderate section (figure 11), the complex visual group (30.3 km/h [18.8 mi/h]) is significantly slower than all other groups ($F = 14.59$, $df = 6/84$, $p = 0.0001$).

In general, the complex visual is slower than the other groups; these differences increase over loading and subzone.

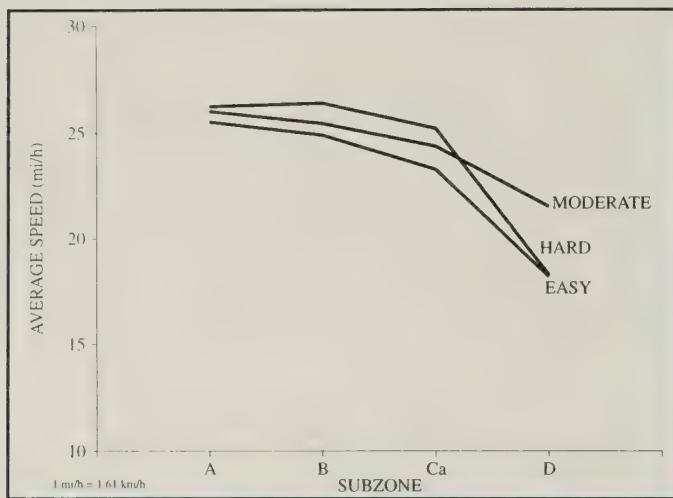


Figure 13.—Average speed broken down by subzone and loading, younger only.

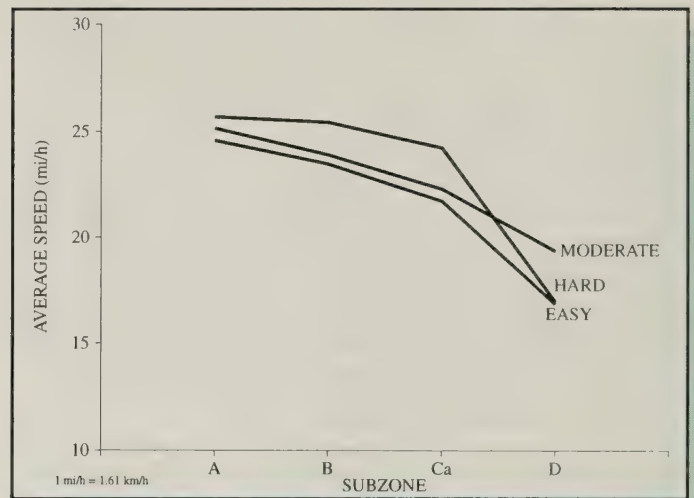


Figure 14.—Average speed broken down by subzone and loading, middle only.

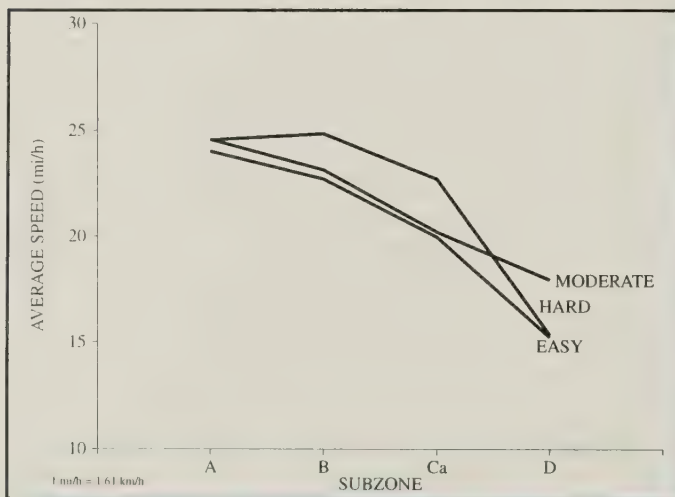


Figure 15.—Average speed broken down by subzone and loading, older only.

There is an overall age group effect ($F = 17.21$, $df = 2/84$, $p = 0.0001$) in which—as expected—the younger drivers are fastest (37.96 km/h [23.59 mi/h]), then the middle-aged drivers (35.69 km/h [22.18 mi/h]), and the older drivers are slowest (33.66 km/h [20.92 mi/h]). These averages are for the turn zones, collapsed across loading sections and subzones.

There are also interactions of age group with subzone ($F = 5.32$, $df = 6/252$, $p = 0.0001$), and with loading and subzone ($F = 2.32$, $df = 12/504$, $p = 0.0069$). Figures 13, 14, and 15 show these interactions.

Between A and B, the older and middle-aged groups slow significantly more ($F = 6.98$, $df = 2/84$, $p = 0.0016$) than the younger group. Speed reductions are 1.30, 1.38, .56 km/h (0.81, 0.86, and 0.35 mi/h), respectively. Between B and Ca, the older group slows significantly more ($F = 16.08$, $df = 2/84$, $p = 0.0001$) than the middle-aged and younger groups. Here the reductions are 4.20, 2.46, 2.09

km/h (2.61, 1.53, and 1.30 mi/h), respectively. The two most significant contrasts related to the age-by-loading-by-subzone interaction are as follows:

1. Comparing changes from A to B in the easy versus moderate, the older group slows more than the other two groups ($F = 8.59$, $df = 2/84$, $p = 0.0004$). Even though all groups slow more in the moderate than in the easy section, the older group shows twice the effect of the younger group, with the middle group in between. Changes are 2.55, 1.19, 1.61 km/h (1.71, 0.74, and 1.00 mi/h), respectively.
2. Comparing changes from B to Ca in the easy section versus the moderate section, the results are similar ($F = 5.24$, $df = 2/84$, $p = 0.0072$), except that the middle group is not different from either of the others. For the younger group, the slowing in the moderate section was actually less than in the easy section, so their average contrast is -0.23 km/h (-0.14 mi/h). For the middle and older groups, the averages were .68 and 1.30 km/h (0.42 and 0.81 mi/h), respectively.

Although these amounts are small, they are in addition to the overall age effects and the age-by-subzone effect. Moreover, the pattern of interactions emphasizes the additional problems experienced by the aging driver.

Speed in Cb

Compared to the other groups as a whole, the simple groups differ only in subzone Ca, where they are faster. But this difference is only an artifact of splitting subzone C into Ca and Cb for the simple groups. The drivers had to slow most in the 61 m (200 ft) immediately before the turn, and these data are included in C (labeled Ca) in the other five groups. Comparing the two groups to each other, there were no treatment effects, even

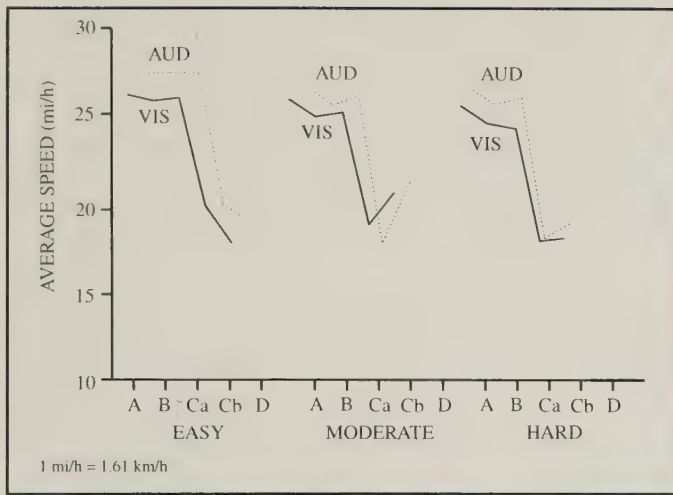


Figure 16.—Average speed for simple visual and simple audio devices, broken down by loading and subzone.

though the simple audio group was faster in 12 of the 16 subzones (figure 16).

As in the larger speed analysis, there were significant age-group ($F = 8.43$, $df = 2/24$, $p = 0.0017$), loading ($F = 6.34$, $df = 2/48$, $p = 0.0036$), subzone ($F = 296.75$, $df = 4/96$, $p = 0.0001$), and loading-by-subzone ($F = 31.51$, $df = 8/192$, $p = 0.0001$) effects. In addition, there was a significant age-by-subzone effect ($F = 3.77$, $df = 8/96$, $p = 0.0022$).

The loading profile indicated no significant differences between the easy and moderate sections, nor between the moderate and hard sections. Therefore, the overall significance noted must be based on a significant difference between the easy and hard sections, indicating a minor overall loading effect for the simple groups.

The subzone profile indicated no significant slowing between B versus Ca or Cb versus D (overall loading sections). As in the larger speed analysis, there is a significant drop from A to B ($F = 34.61$, $df = 1/24$, $p = 0.0001$). As in the larger analysis, there is more slowing in the moderate and hard sections than in the easy section ($F = 9.85$, $df = 1/24$, $p = 0.0001$). As mentioned before, a possible reason for this is that the gas-mileage problems were more difficult in the moderate and hard sections.

The largest effect in the entire analysis is the difference between Ca and Cb ($F = 418.09$, $df = 1/24$, $p = 0.0001$), with an average slowing of 11.3 km/h (7.0 mi/h). Unfortunately, in retrospect it can be seen that the effect of the navigational message is confounded with the effect of subjects slowing for the turn; these cannot be separated in the absence of Cb speed data for the other groups.

Another large effect occurs in the contrast analyses for loading-by-subzone interactions. Comparing the easy to the moderate section, note

the change from Cb to D. In the easy section, the drivers slowed by 2.7 km/h (1.7 mi/h); in the moderate section, their speed in the last subzone (D) was faster than in subzone Cb by 4.3 km/h (2.7 mi/h). The hard section was more similar to the moderate than the easy section, although the increase in speed from Cb to D was only 1.0 km/h (0.6 mi/h). It is logical that speeds in subzone D were higher than those in subzone Cb, as D is longer and drivers had more time to regain their normal speed.

The age-group-by-subzone interaction was also similar to those discussed previously. The largest age effects occurred in subzone Cb, especially in the moderate and hard sections, where the older subjects drove significantly slower than the middle-aged subjects, who drove significantly slower than the younger subjects.

Channel and complexity analysis. An additional analysis was computed for the speed data that deleted the map control group and separated the other six groups into a channel-by-complexity matrix. The two channels were visual and auditory, and the three complexities were simple, medium, and complex. Thus the design had six factors: channel, complexity, age group, sex, loading, and subzone. The analysis did not include the straight zones. As in the original speed analysis, there were significant effects for age ($F = 11.74$, $df = 2/72$, $p = 0.0001$), loading ($F = 60.05$, $df = 2/144$, $p = 0.0001$), subzone ($F = 700.71$, $df = 3/216$, $p = 0.0001$), and loading-by-subzone ($F = 122.41$, $df = 6/432$, $p = 0.0001$).

Also, both the complexity factor ($F = 17.53$, $df = 2/72$, $p = 0.0001$) and the channel factor ($F = 13.42$, $df = 1/72$, $p = 0.0005$) were significant. There was a channel-by-complexity interaction, in conjunction with subzone ($F = 5.43$, $df = 6/216$, $p = 0.0001$). Other interactions not already covered in the original speed analysis include a loading-by-complexity effect ($F = 8.43$, $df = 4/144$, $p = 0.0001$), a subzone-by-channel effect ($F = 12.26$, $df = 3/216$, $p = 0.0001$), a subzone-by-complexity effect ($F = 16.42$, $df = 6/216$, $p = 0.0001$), and a loading-by-subzone-by-complexity effect ($F = 2.36$, $df = 12/432$, $p = 0.0059$).

The loading-by-complexity interaction occurred between the moderate and hard sections. All groups were slower in the hard section, but the complex groups slowed by more than twice as much as the others showing that increased load had more effect on the complex groups, as was expected.

The contrasts indicate that the loading-by-subzone-by-complexity effect only occurs when comparing subzones between the easy and moderate

sections. Inspection of the changes involved indicate that the major cause is the increase from B to Ca in the moderate section for the simple groups, when they show no difference in the easy section, and the other groups slow from B to Ca in both sections. No explanation is offered for this effect.

Regrading the subzone-by-channel-by-complexity effect, inspection of the means—especially comparing the audio groups to their visual counterparts—shows that the simple and medium groups show consistent audio-visual differences, but the complex visual group shows increasing differences from the complex audio group as the subzones progress. This finding leads to the conclusion that loading interacts with complexity and channel at the higher levels. Perhaps the complex visual device simply has too much to distract the driver.

Lateral placement

*Variance of lateral placement.*³ The lateral placement variance measure includes the leeway adjustment based on the changing lane width of the drive. In real numbers, the subjects' performance is quite similar under the three workload conditions. However, because the lanes become narrower, similar variability results in more dangerous driving.

The variability of subjects' lateral placement (relative to leeway) increased as a function of workload in the three sections of the drive. Contrast tests of this variable indicated that variance was higher in the hard than in the moderate section ($F = 62.47$, $df = 1/84$, $p = 0.0001$), and higher in the moderate section than in the easy section ($F = 84.14$, $df = 1/84$, $p = 0.0001$).

The effect of loading was influenced by subzone ($F = 15.60$, $df = 6/504$, $p = .0001$). In the easy section, the effect appears quite small ($F = 63.25$, $df = 3/252$, $p = 0.0001$), but is statistically significant in each subzone. Variance decreases from subzone A to B ($F = 10.66$, $df = 1/84$, $p = 0.0016$).

This decrease is possibly the effect of the stimulus presentation following the very low workload levels of those portions of the drive preceding the B subzone. Hearing the gas mileage problem may have increased subjects' overall attention level. A sudden auditory stimulus demands attention, and may add sufficient short-term workload to improve performance.

Variance continues to increase in subzone Ca ($F = 18.36$, $df = 1/84$, $p = 0.0001$), and increases again following the turn in subzone D ($F = 61.85$, $df = 1/84$, $p = 0.0001$). The magnitude of the latter result appears to be an artifact related to the HYSIM itself. Subjects tended to turn wide, and did not begin to make corrections until near the end of the turn.

The moderate section variance pattern is almost identical. The decrease from A to B in the lateral placement variance measure ($F = 34.11$, $df = 1/84$, $p = 0.0001$), although it appears inconsistent with the workload hypothesis, is interpretable in light of the average lateral placement result for the same subzone. Lane placement tended to "worsen" in that subjects did not stay centered in the lane. However, they tended to keep their vehicle positioned away from the other car. Thus at this level of workload, performance in this subzone was reasonably stable. In contrast, in the hard section variance increases from A to B, which may reflect the load of a difficult gas mileage problem, added to an already high workload situation. Though the trend is clear, this result is not significant.

Lane placement variance was also affected by an interaction of subzone and age group ($F = 4.36$, $df = 6/252$, $p = 0.0001$). This significant effect is due to the larger variance scores of the older group in subzone D (figure 23).

Sex emerged as a significant factor in interaction with subzone ($F = 6.17$, $df = 3/252$, $p = 0.0056$; see figure 24), as well as with both subzone and loading ($F = 5.73$, $df = 6/504$, $p = 0.0049$). This sex interaction may be due to a phenomenon often found in older groups with no upper age limit, by which the women are older, on average, than the men. Further investigation of this possibility did, in fact suggest that these female-male differences were related to age differences.

No significant treatment effects were found in the analysis of lateral placement variance. Separate analyses of the simple groups, thus, showed the same pattern of changes in subzones A, B, Ca, and D. The Ca to Cb changes appear to capture the subjects' preparation for the upcoming turn; this is particularly suggested in the loading-by-subzone interaction ($F = 29.17$, $df = 2/48$, $p = 0.0001$), in which there was a greater decrease in lateral placement variance in the hard section than in the easy ($F = 38.83$, $df = 1/24$, $p = 0.0001$), and moderate ($F = 32.65$, $df = 1/24$, $p = 0.0001$)

³Note that certain of the subzone lateral placement data seemed consistent with the rest and were consequently deleted.

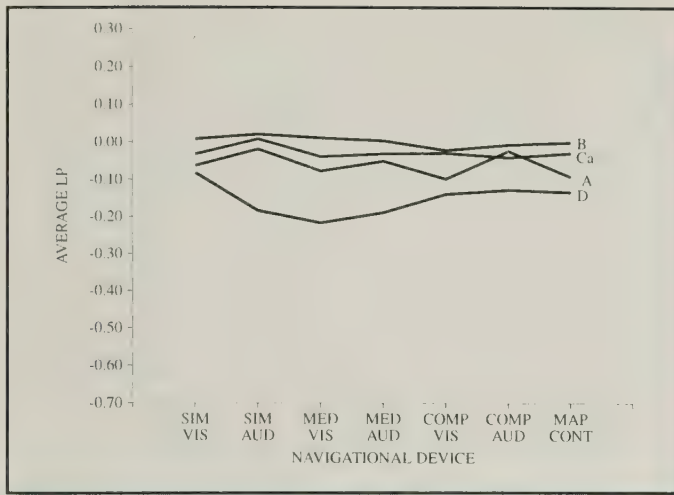


Figure 17.—Average lateral placement (LP) broken down by subzone and treatment, easy loading only.

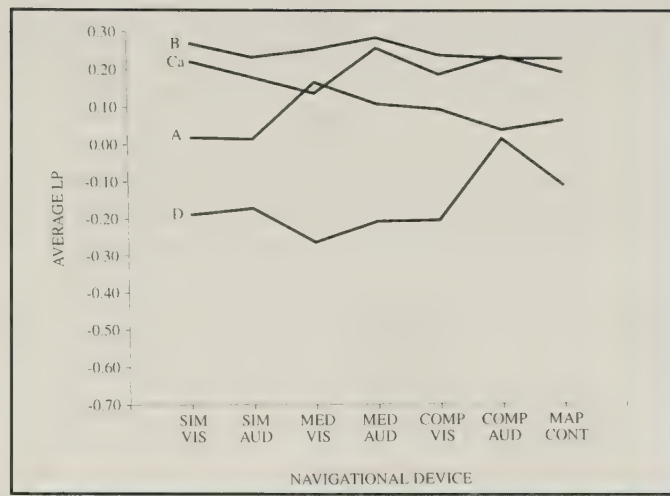


Figure 19.—Average lateral placement (LP) broken down by subzone and treatment, hard loading only.

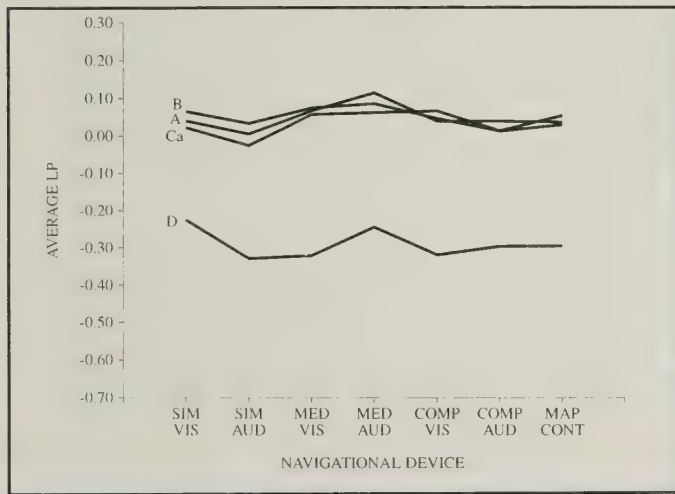


Figure 18.—Average lateral placement (LP) broken down by subzone and treatment, moderate loading only.

sections. The subzone interaction is due primarily to the larger decrease in variance from Ca to Cb in the hard section. The increased workload level apparently caused a higher level of lateral placement variance in the hard section Ca subzone relative to the easier sections of the drive. Thus the decrease from Ca to Cb is greater in that section as subjects anticipate the turn.

Average lateral placement. The average lateral placement data are presented in figures 17, 18, and 19. The same vertical scale has been used in all three figures to emphasize the differences among the loading sections. Again, the differences in the unadjusted lane placements were fairly equal. However, the leeway-adjusted scores, which are pictured, emphasize the increase in danger between loading sections.

The most salient effect in the data was a subzone effect ($F = 363.41$, $df = 3/252$, $p = 0.0001$). When the data were averaged over treatment, the order of the subzones was quite invariant. Subzone B was always the most positive, then subzone Ca,

and subzone A; subzone D was always the most negative. Even when the data were broken down by loading section this order remained, and the profile analyses (which compared A to B, B to Ca, and Ca to D) were all significantly different at the $p = 0.0001$ level. To determine whether subzone A was different from subzone Ca, another set of analyses was run using a contrast between A and the other subzones. With one exception (moderate A versus moderate Ca), these were also significant, usually at the $p = 0.0001$ level.

An analysis compared Cb to Ca (for the simple groups) and found no effects except a loading effect similar to that in the overall analysis. Thus, unlike average speed and lateral placement variance, there were no changes in average of lateral placement as subjects in the simple groups drove from Ca to Cb.

There is a plausible explanation as to why subzone D was always most negative: Drivers tended to cut off too little of the corners at the beginning of a turn, which placed them wide of the mark in subzone D. In the moderate and hard sections, drivers sometimes were so far in the other vehicle's lane that when it reappeared, it did so directly in front of them. Older drivers were more likely to experience this, which accounts for a significant subzone-by-age-group effect ($F = 10.31$, $df = 6/252$, $p = 0.0001$).

Concerning subzone B, in the easy section the average lateral placement was closest to the middle of the lane; in the moderate and hard sections it was farthest away from the other vehicle. Subzone B thus could be considered the safest subzone. Just as in the variance of lateral placement, the gas mileage question is thought to have improved the driver's attention level, thus improving performance in subzone B.

The subzone effects for A and Ca are not as explainable. In the moderate and hard sections, average lateral placement in Ca was closer to the middle of the lane than in B; thus, the drivers were better placed for the turn. This fact does not apply in the easy section where drivers are slightly wide before the turn, unless they started wide so they would not have to cut off as much of the corner.

In the moderate and hard sections of subzone A, the average is closer to the middle of the lane than any of the other subzones. A possible explanation is that if drivers are less attentive, centering themselves in the lane is a more automatic driving response than staying away from the other vehicle. However, this explanation does not apply in the easy section, where the drivers were slightly negative in subzone A.

It is true that one of the two situations where there was a treatment effect was in subzone A of the easy section, and the map control and complex visual groups, which knew the direction of their turn at subzone A, were significantly more negative than the simple audio group, which did not know the direction of the next turn. In this sense the map control and complex visual groups could have been swinging wide before the turn as was posited for all groups in subzone Ca of the easy section. Unfortunately, the complex audio group—the other group that knew the turn direction by subzone A—did not fit this pattern at all.

In subzone D of the hard section, the complex audio group was closer to the middle of the lane than any other group, and significantly closer than the medium visual group. No explanation is presented for this effect.

A minor loading effect was observed ($F = 5.51$, $df = 2/168$, $p = 0.0048$), in which the lateral placement (collapsed across subzones) was more negative for the easy section than for the moderate section; there were no differences between the moderate and hard sections. This circumstance is easily explained by the introduction of the other vehicle in the moderate zone. With no oncoming traffic, the drivers set their average lateral placement slightly away from the car or truck that was shadowing them.

Discussion and Conclusions

The results of this study are subject to several caveats:

1. Because the devices simulated in this study do not now exist on the commercial market no comparisons should be inferred regarding devices currently in use.

2. Although the simulation conducted in this study provide a baseline scenario, generalization to real-world driving is limited by the constraints of the situation (i.e., only a nighttime scene was used, only one other vehicle was present, and the environment was visually and auditorially sparse.)
3. The samples used in this study—particularly the older subjects—cannot be taken as representative of actual populations. Moreover, a variety of subject responses as reactions during the course of the study may have skewed the findings.

Age effects

In general, the older drivers performed less safely. They drove more slowly, had larger variability in lateral placement, had longer reaction times to the gauges, were more likely to be in the other vehicle's lane after the turn, and were more likely to make navigational errors compared to the other two age groups.

The age factor interacted to a great extent with the loading factor. This interaction was apparent in reaction time to gauge changes, speed, and both average and variance of lateral placement. Future studies must include both factors to adequately determine the response of older drivers in extreme real-world situations. The age data in this study are slightly inconsistent with those generally reported. Usually, older populations have larger within-group variance—that is, they usually have a wider range of abilities. The only variable for which such differentiation occurred was variance of lateral placement. There was no consistent pattern for the other variables.

Treatment effects

The most salient treatment effects occurred with the complex visual device. These effects are closely linked to the safety of driving performance. Subjects in this condition missed more gauge changes, had longer reaction times, and drove more slowly than subjects using any other devices except the strip map. At some points, even subjects using the strip maps performed more safely than the complex visual group.

Note that measures of lateral placement are not included in the above list, possibly because subjects gave lateral placement their highest priority. To maintain lane position—which is so critical to safety—drivers will perhaps sacrifice speed, navigation, and other peripheral tasks. This is consistent with the theory of risk homeostasis (behavioral adaptation).

Navigational Errors

Determining the effectiveness of the navigational devices is essentially a digression from the purpose of this research. However, the subjects made several errors that appeared to be related to the particular device used. These are described below.

Navigational errors were first screened for those caused by either the experimenters or equipment faults, and for those which resulted from the combined idiosyncrasies of a particular device with some aspect of the experimental apparatus or scenario. These errors were not included in the final error count (see table 2).

Responses in a turn zone were counted as errors if the subject drove beyond, turned before, or turned the wrong direction at the correct intersection.

Chi square analysis, based on number of correct turns versus errors for each device, was significant. These results should be viewed with caution, however, because they are based on repeated measures rather than independent observations. This caveat notwithstanding, the devices appear to fall into three categories:

- Lowest number of errors—simple audio, medium audio, and medium visual.
- Medium number of errors—complex audio.
- Highest number of errors—map control, complex visual, and simple visual.

The simple audio group performed much better than the simple visual group, probably because the spoken message attracted more attention in the quiet environment of the HYSIM. Driving requires constant processing of visual information, and thus the single arrow may be an insufficient cue under routine workload conditions.

Of the two complex systems, subjects made fewer errors with the audio device. Hearing the name of the street periodically during the drive appeared to be more useful than either a paper map or a dynamic map display. Subjects in the complex visual group seemed less dependent on street signs, as they made no more errors at the hidden sign intersection than at others. It is possible that some subjects simply had trouble in correctly identifying the correspondence between the electronic map and the roads in the HYSIM. If so, this problem may be exacerbated on actual roadways, which are naturally much more complex than can be reproduced in the HYSIM.

Table 2.—Frequency of navigational errors

Device	Errors
Simple	
Visual	16
Audio	0
Medium	
Visual	3
Audio	1
Complex	
Visual	12
Audio	8
Map control	14

Auditory versus visual devices. Subjects using the three auditory devices did not reduce their speeds as much as did those using the three visual devices during high load situations. Also, they made fewer navigational errors than those using visual devices.

Device complexity. Subjects using the complex devices drove more slowly than those using the other devices. The only difference between the simple and medium devices was that those using the simple visual device made a large number of navigational errors. Overall, it is suspected that the redundancy offered by the medium devices would result in safer driving in the real world. The medium devices take advantage of human factors principles by providing the optimal amount of information at the proper time. (5) Several subjects—especially older drivers, commented that the complex devices (both visual and audio) gave too much information. Future studies should add medium complexity devices that combine both auditory and visual channels, such as ERGS and AUTOGUIDE.

References

- (1) H.T. Zwahlen, C.C. Adams, Jr., and P.J. Schwartz. "Safety Aspects of Cellular Telephones in Automobiles." Paper presented at the 18th International Symposium on Automotive Technology and Automation, Florence, Italy, June, 1988.
- (2) J. Walker, E. Alicandri, C. Sedney, and K. Roberts. *In-vehicle Navigation Devices: Effects on the Safety of Driver Performance.* Publication No. FHWA-RD-90-053, Federal Highway Administration, Washington, DC, May, 1990.

(3) General Motors Research Laboratories & Delco Radio Division, GMC, *A Design for an Experimental Route Guidance System, Vol. 1: System Description*, Report No. GMR-815-I, prepared for the Federal Highway Administration, Washington, DC, November, 1968.

(4) Federal Highway Administration, *Manual on Uniform Traffic Control Devices*, Revised Edition, Washington, DC, March 1986.

(5) G.J. Alexander and H. Lunenfeld. *Positive Guidance in Traffic Control*. Federal Highway Administration, Washington, DC, April 1975.

Jonathan Walker is a senior experimental psychologist at COMSIS, Corporation, Silver Spring, Maryland. Between 1984 and 1991, he conducted research in the FHWA Human Factors Laboratory at the Turner-Fairbank Highway Research Center under a support contract. Before that, he taught experimental psychology at King College, Bristol, Tennessee. He holds a doctoral degree from the University of Virginia.

Elizabeth Alicandri is an engineering psychologist in the Information and Behavioral Systems Division of the Federal Highway Administration's Office of Safety and Traffic Operations, R&D. She has participated in human factors highway safety research since 1984, when she began working in the Turner-Fairbank Highway Research Center's Human Factors Laboratory as a Research Fellow.

The research reported here was performed while she was working as onsite contract support staff for the human factors laboratory. Her current highway safety research areas include driving simulation, older drivers, and IVHS.

Catherine A. Sedney is a research psychologist in the Human Performance Technology Division of SAIC. She has participated in human factors research since 1986. The research reported here was performed while she was working for COMSIS Corporation as on-site contract support staff for the human factors laboratory. Her current highway safety research areas include useful peripheral vision and IVHS.

King M. Roberts is the Manager, Human Factors Laboratory, FHWA Office of Safety and Traffic Operations R&D. Since 1974, he has worked in transportation research with specific emphasis on delineating the performance capabilities and limitations of drivers. The current focus of this work is in IVHS.



Rock Riprap for Protection of Bridge Abutments Located at the Flood Plain

by Jorge E. Pagán-Ortiz

Introduction

Bridge abutments commonly contract the free flow of water in the channel and flood plains through the bridge opening during high flows. During high flow events, the abutments are subject to strong erosive currents that are forced to pass through the bridge opening. These currents undermine the streambed at the toe of the abutments and beyond. This phenomenon, known as local scour at the abutments, in turn causes acceleration of flow deflected by the abutments. The development of a vortex system induced by the obstruction is the principal mechanism for the development of local scour. The strength of the vorticity generated by the deflection is related to the depth of flow, abutment depth and shape, alignment of the abutment with respect to the flow, size of bed material, rate of bed material transportation, and ice or drift accumulation.

Laboratory measurements indicate that average point velocities away from the abutment area are not influenced by the abutment's presence. Consequently, scour at abutments is considered a local phenomena that is not significantly related to the overall geometry of the flow. (1)¹

A common method for protecting the stream bed from erosive currents is to place a rock riprap apron. To determine the size of rock riprap needed to prevent local scouring at abutments, it is necessary to study the stability of the rock as it is exposed to the erosive currents in the channel and flood plain.

This study was conducted at a hydraulic flume of the Federal Highway Administration Turner-Fairbank Highway Research Center. Results of this study are presented in this article. Complete results of the study are presented elsewhere. (2,3)

Literature Review

Many researchers have developed equations based on average velocity that relate the critical conditions affecting stability. Isbash presented an equation that can be expressed as: (4)

$$N_{sc} = E^2 * 2 \quad (1)$$

where:

N_{sc} = sediment number representing the ratio of approach flow inertial energy at critical conditions

¹Italic numbers in parentheses identify references on pages 30-31.

to the stabilizing potential created by the submerged rock weight. (5)

For loose stone lying on top of the fill, N_{sc} is expressed as:

$$N_{sc} = \frac{V^2}{[g * D_{50} * (SG - 1)]} \quad (2)$$

where:

- V = flow velocity that will remove the loose stones m/s(ft/s)
- D_{50} = characteristic median rock size m(ft)
- SG = Specific Gravity of the rock
- g = gravitational acceleration 9.8m/s²(32.2 ft/s²)
- E = 0.86 for loose stone lying on top of the fill

For stones deposited into flowing water that roll (due to the force of water acting over them) until they find a "seat" and a support, $E = 1.2$.

Rearranging equation 2 in terms of D_{50} for $E = 1.2$, we obtain:

$$D_{50} = \frac{0.347 * V^2}{(g * (SG - 1))} \quad (3)$$

Equation (3) is a rearranged form of the Isbash equation.

Neill established a relation for "first displacement" of uniform graded gravel based on uniform parameters. (6) The following expresses conservative design curve:

$$N_{sc} = 2.50 * \left(\frac{D_g}{d}\right)^{-0.20} \quad (4)$$

where:

- D_g = characteristic rock size on the approach flow bed m(ft)
- d = depth of the approach flow m(ft)

Parola conducted experiments using Neill's criteria for first displacement and found good agreement. (5) Figure 1 shows the sediment number curve, N_{sc} , based on Neill's and Parola's experiments for unobstructed flow—no obstruction to the free flow of water.

Pagán developed the following regression equation for an average sediment number design curve based on Neill's and Parola's experiments for undisturbed flow: (2)

$$N_{sc} = 2.58 * \left(\frac{D_g}{d}\right)^{-0.27} \quad (5)$$

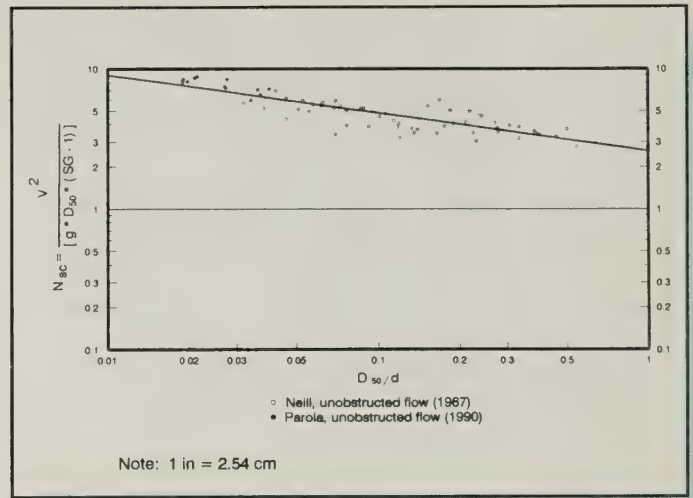


Figure 1.—Sediment number curve for unobstructed flow.

Framework of Experiments

The parameters that characterize the disturbed flow are:

- V_{cc} = average velocity of the contracted flow at observed incipient motion of the rock at the contraction m(ft/s)
- d_{cc} = average depth of the contracted flow at observed incipient motion of rock at the contraction m(ft)
- W_a = width of the approach flow m(ft)
- W_{t-c} = width of the contraction m(ft)
- D_{50} = characteristic median rock size on the contraction flow bed m(ft)
- AS = factor associated with the abutment shape
- K = roughness of the bed upstream
- K_s = roughness of the bed surrounding the obstruction
- g = gravitational acceleration 9.8 m/s² (32.2ft/s²)
- ρ = fluid density 998.2 kg/m³ (1.93 slugs/ft³) @20°C
- ρ_s = rock density (kg/m³)
- μ = dynamic viscosity of fluid kg/m-s(slug/ft-s)

The effect of displacement due to leaching of fines through the armored apron of gravel in the observation area near the toe of the abutment and flood plain was not studied. The size of the bed material, D_{50} , in the obstructed area and the roughness in the vicinity of the obstruction, K_s , are dependent variables. For the purpose of the experiments, K_s was assumed to be adequately represented by D_{50} .

The characteristic parameters can be arranged into a functional equation that describes the critical condition for the initial motion of the rock as follows:

$$0 = f(W_a, W_{t-c}, d_{cc}, D_{50}, V_{cc}, AS, K, g, \rho, \rho_s, \mu) \quad (6)$$

The parameter, g , must appear in combination with ρ and ρ_s as follows:

$$\gamma = g * (\rho_s - \rho) \quad (7)$$

Combining equations (6) and (7) in non-dimensional form yields the following:

$$N_{SC} = f(V_{cc} * \frac{D}{v}, \frac{\rho_s}{\rho}, \frac{d_{cc}}{W_{t-c}}, \frac{D_{50}}{d_{cc}}, AS, \frac{W_a}{W_{t-c}}, K) \quad (8)$$

where:

N_{sc} is defined in equation (1)

$v = \mu/\rho$.

D = characteristic rock size (assumed to be adequately represented by D_{50}).

Yalin stated that (ρ_s/ρ) "can be important only with regard to the properties associated with the 'ballistics' of an individual grain." (6)

In case of highly turbulent flows needed to cause the initial motion of the rock protection, the influence of the obstruction particle Reynolds number—the effect of viscosity relative to inertia, $V_{cc} * (D/v)$, was considered to be negligible because it was greater than 10^3 , which is well beyond the range that Shields and other researchers found to be no longer a factor.

Therefore, by applying the preceding considerations and confining the research to subcritical flow, the effect of (ρ_s/ρ) , and $[V_{cc} * (D/v)]$ can be discounted. Thus, equation (8) can be reduced as follows:

$$N_{SC} = f(\frac{d_{cc}}{W_{t-c}}, \frac{D_{50}}{d_{cc}}, AS, \frac{W_a}{W_{t-c}}, K) \quad (9)$$

By using the contracted velocity in N_{sc} , the effect of d_{cc}/W_{t-c} , W_a/W_{t-c} , and K are negligible. Thus, equation (9) reduces to:

$$N_{SC} = f(\frac{D_{50}}{d_{cc}}, AS) \quad (10)$$

Equation 10 provides the framework used to determine the stability of rock riprap to protect the toe of an abutment at the flood plain. The quantity N_{sc} is defined in equation (1). The parameter D_{50}/d_{cc} represents the relative roughness of the contracted flow.

Experimental Model

Two small scaled abutment models, vertical-wall and spill-through, were used to study the impact of the abutments on time-averaged contraction velocities and the stability of gravel placed around the toe of the abutment and flood plain. The

length of the abutment was varied to investigate the effect of the contraction to the flow on the flood plain. For the vertical-wall abutment model, the length ranged from 127 to 508 mm (5 to 20 in); for the spill-through abutment model, the length ranged from 635 to 1 016 mm (25 to 40 in). The total width of the vertical-wall and spill-through abutment was 152.4 and 1 168.4 mm (6 to 46 in), respectively. Flow depths ranged from 46.7 to 266.7 mm (1.84 to 10.5 in).

Observation Area

An observation area was defined in the hydraulic flume for each abutment model to visualize the failure of gravel for a given flow. These areas are illustrated in figures 2 and 3.

Gravel Placement

Two different sizes of gravel were used in the experiments: $D_{50} = 7.62$ mm (0.30 in) and 10.2 mm (0.40 in). The gravel were angular particles that passed one sieve and were retained on the next

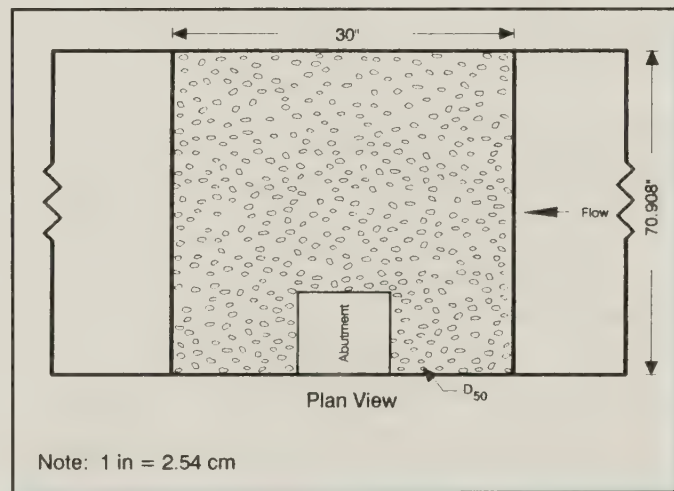


Figure 2.—Observation area for vertical-wall abutment.

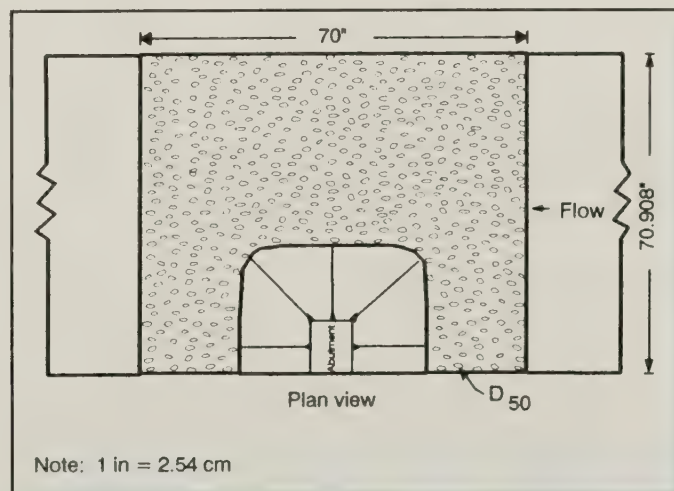


Figure 3.—Observation area for spill-through abutment.

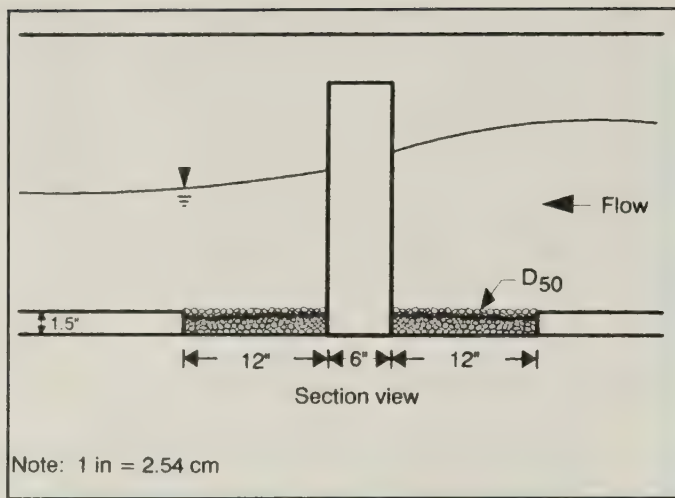


Figure 4.—Section view of the gravel setup for vertical-wall abutment.

standard size so they were intended to be uniform in size. The gravel was placed in the observation area to a depth of 38.1 mm (1.5 in) in three non-uniform layers. The intermediate layer was spray-painted red to help visualize the failure or motion of the upper gravel layer. Figures 4 and 5 illustrates a typical gravel setup for each abutment model. Gradation and layer thickness were not variables in these experiments.

Experimental Procedure

The experimental procedure for each run was as follows:

1. Discharge was set to a constant.
2. Tailgate was raised to develop a velocity past the observation section slightly below the expected incipient velocity of the rock riprap failure.
3. Tailgate was gradually lowered until a discernible patch of surface rock moved in the observation section. This was determined by looking for a visible section of the colored underlying layer of rock.
4. Flow and the tailgate setting were then held constant while a grid of depth and velocity measurements were taken. This generally took approximately one and a half hours. Very few additional particles moved during this data collection period; so, it was felt that longer run times would not have changed the results.

Experimental Results

Independent experiments were conducted with each abutment model to determine the vulnerable zone for the gravel failure within the observation area at different discharges and flow depths. An initial zone of failure thus was identified for each model.

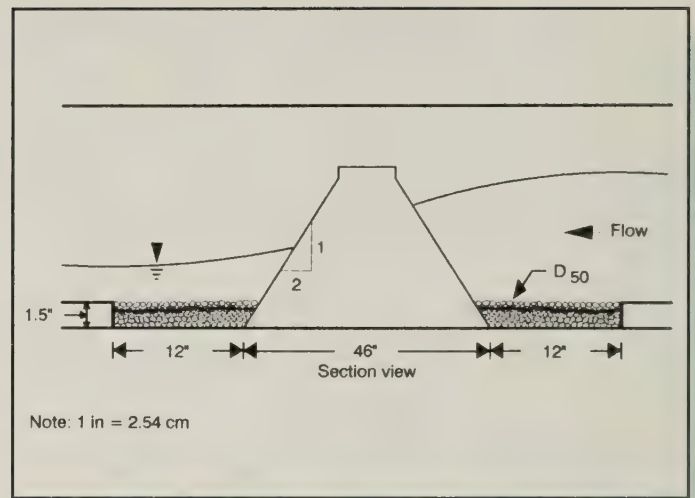


Figure 5.—Section view of the gravel setup for spill-through abutment.

Previous research have demonstrated that the scour hole pattern in an unprotected channel and flood plain being obstructed by either a vertical-wall or spill-through abutment normal to the flow occurs at the upstream corner of the abutment. (7) Pagán demonstrated that the failure zone in an armored flood plain surrounding the abutment normal to the flow is a function of the abutment shape. (2,3)

For the *vertical-wall abutment* model the initial failure zone was consistently observed at the upstream corner of the abutment in the armored flood plain (figure 6). The zone then expands downstream toward the abutment and away from it with time and increase in discharge.

For the *spill-through abutment* model, the initial failure zone was consistently observed at the downstream radius of the model just away from its toe (figure 7). The zone then expands downstream and upstream toward the toe of the abutment and away from it into the flood plain with time and increase in discharge.

Velocity-Based Criteria

Three equally spaced average point velocities were measured within the contraction zone. For the smooth bed experiments (no gravel placed within the observation area) it was learned that the readings of average point velocities near the face of the abutment parallel to the flow were severely affected by the flow turbulence. Consequently, low velocity readings were measured near the face of the abutment. The same result was obtained in the obstructed flow experiments (free flow of water obstructed by an abutment) with gravel placed in the observation area. However, the gravel was failing at the upstream corner of the vertical-wall abutment (figure 6) and down-

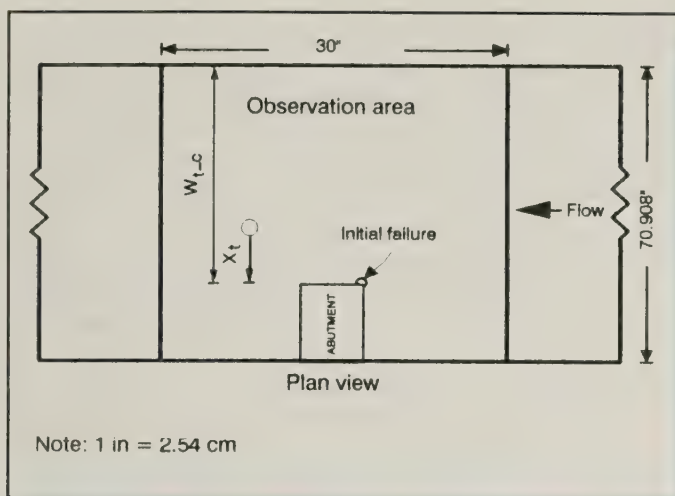


Figure 6.—Location of initial failure zone for vertical-wall abutment.

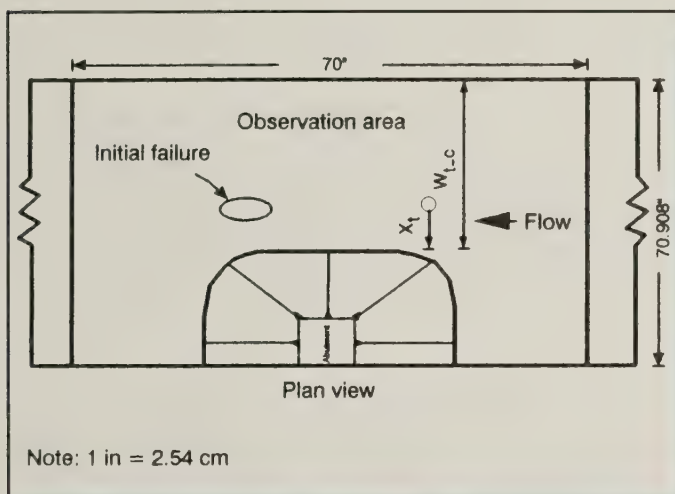


Figure 7.—Location of initial failure zone for spill-through abutment.

stream near the toe for the spill-through abutment (figure 7). Thus, although the flow turbulence affected the velocity readings near the abutment models, that velocity has to be much higher than those measured during the experiments to cause the initial motion of the gravel near the toe of the abutment models.

Vertical-Wall Abutment

The vulnerable zone for incipient motion for this abutment model was observed at the upstream corner of the abutment (figure 6). The separation of flow created by the contraction of the abutment caused a strong turbulence, particularly for deeper flows. With the flow depth and velocity at the approach and for a computed discharge representing the design discharge, the velocity and flow depth were computed at the contraction of the abutment in the flood plain using Bernoulli's energy equation without elevation terms (11) and

Continuity equation (12). The energy equation is as follows:

$$\frac{V_{am}^2}{2 * g} + d_a = \frac{V_{cc}^2}{2 * g} + d_{cc} + h_L \quad (11)$$

where:

V_{am} = measured average point velocity at the approach m (ft/s)

d_a = measured average depth at the approach m (ft)

V_{cc} = computed average point velocity at the contraction for disturbed flow m/s (ft/s)

d_{cc} = computed average depth at the contraction for obstructed flow m (ft)

h_L = energy losses (assumed to be negligible) m(ft)

g = gravitational acceleration 9.8 m/s² (32.2 ft/s²)

The Continuity equation is as follows:

$$Q_{cc} = V_{cc} * W_{t-c} * d_{cc} \quad (12)$$

where:

Q_{cc} = computed discharge (cfs)

W_{t-c} = horizontal distance (ft) from the toe of the abutment to the channel boundary as shown in figures 6 and 7

Using equation (2), the sediment number, N_{sc} , was computed for V_{cc} . The values of N_{sc} were plotted against the D_{50}/d_{cc} ratio. Figure 8 shows a plot of the individual computed sediment number curve for the vertical-wall abutment model for $D_{50} = 7.62$ mm (0.30 in) and 10.16 mm (0.40 in) for obstructed flow.

This figure also shows that the curves for the two gravel sizes, which were derived by regression, were close to one curve and almost parallel to the unobstructed flow curve (figure 1). The velocity, V_{cc} , is the computed average contracted velocity within the flood plain for the obstructed flow, but observed failure is for any discernible area of particular movement in that opening.

Figure 9 shows the combined sediment number curve for the two gravel sizes. This plot reveals that the slope of the combined curve follows that of the unobstructed flow curve. For the gravel to fail at the toe of the abutment upstream of the constriction, the local effective velocity must have been close to that that would have caused failure for the unobstructed flow curve.

Flow at the upstream corner of the abutment where the initial failure of rock riprap occurred was highly rotational and was difficult to quantify with the electromagnetic probe sensor, the instrumen-

tation available for this study. The so called "local effective velocity" is defined as the velocity that would have moved the rock in unobstructed flow.

To determine the stable size of rock riprap, equation (2) should be rearranged as follows:

$$D_{50} = \frac{V_{cc}^2}{g * N_{sc} * (SG - 1)} \quad (13)$$

where:

V_{cc} = computed average velocity at the contraction within the flood plain m/s (ft/s)

By regression analysis of the combined sediment number curve (figure 9), N_{sc} is obtained as:

$$N_{sc} = 0.94 * \left(\frac{D_{50}}{d_{cc}} \right)^{-0.23} \quad (14)$$

Substituting equation (14) into equation (13) yields:

$$D_{50} = \frac{1.0836 * V_{cc}^{2.598}}{g^{1.299} * d_{cc}^{0.299} * (SG - 1)^{1.299}} \quad (15)$$

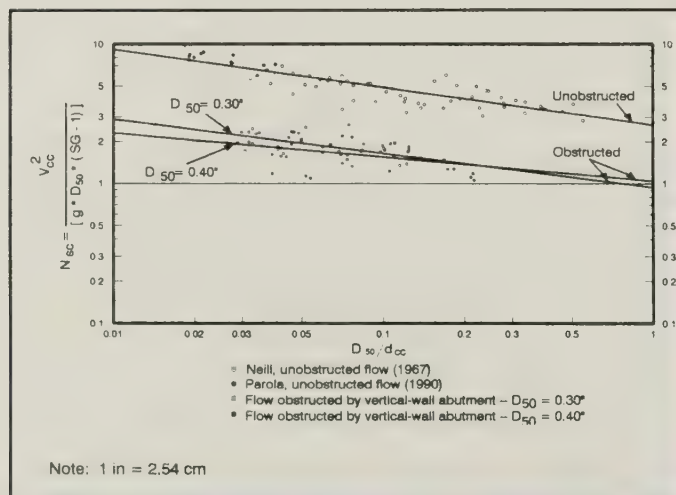


Figure 8.—Individual sediment number curve for vertical-wall abutment.

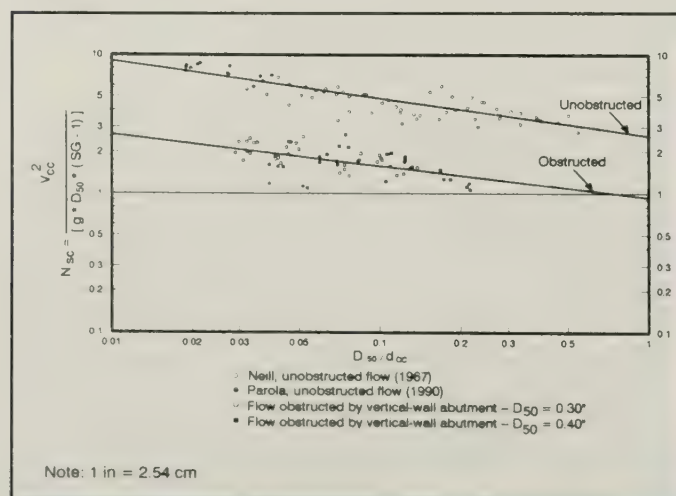


Figure 9.—Combined sediment number curve for vertical-wall abutment.

Although equation (15) is not dimensionless as written, it is dimensionally homogeneous—i.e., can be reduced to the same units on both sides. It can be used with either the International System of units (SI) or English units as long as consistent units are used in all of the terms.

Figure 10 presents a plot of V_{cp} / V_{cc} versus X_t / W_{t-c} . The velocity ratio, V_{cp} / V_{cc} , represents the effective computed local velocity (near the abutment face at which the rock failed) to the computed average contracted velocity in the flood plain within the contraction.

The ratio of V_{cp} / V_{cc} also represents the indirect method—or "simple multiplier"—that should be applied to the computed average contracted velocity in the contraction within the flood plain to obtain the velocity near the abutment face that caused the gravel's incipient motion.

V_{cp} is the computed average point velocity at the contraction for undisturbed flow, in ft/s. V_{cc} is the average computed point velocity at various distances, X_t , from the toe of the abutment for disturbed flow. W_{t-c} is the horizontal distance from the toe of the abutment to the channel boundary, in m (ft). Both X_t and W_{t-c} are shown in figures 6 and 7.

At $X_t / W_{t-c} = 0$, and for 95 percent of the of the computations, the ratio, V_{cp} / V_{cc} , fell near 2.0. At $X_t / W_{t-c} = 0$, and for 5 percent of the computations, the ratio reached 2.304.

The local effective velocity had no resemblance to what actually occurred around the abutment, but it was a convenient parameter to use in developing a simple multiplier ($V_{cp} / V_{cc} = 2.0$) for the velocity term in the rearranged Izbash equation [equation (3)]. The velocity term within equation (3) can be multiplied by 2.0 to compute the rock riprap size for the vertical-wall abutment model.

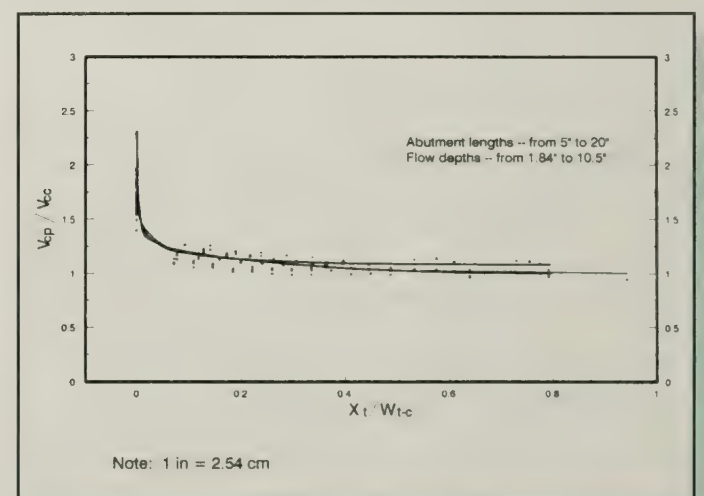


Figure 10.—Point velocity ratio for vertical-wall abutment.

The discharge was increased 1.7 times the discharge that caused the incipient motion of the gravel to observe the extent of the failure zone. The multiplier, 1.7, is suggested to approximate Q_{500} from Q_{100} . (8) This demonstrated that the rock riprap apron should be extended along the entire length of the abutment, both upstream and downstream, and to the parallel face of the abutment to the flow.

Figure 10 also illustrates that the velocity amplification decays rapidly with distance from the toe of the abutment and that the effect of the abutment occurs in a small portion of the contracted area. Therefore, it would be reasonable to limit the rock riprap apron to a relative small portion of the constriction. However, additional data analysis needs to be made to determine the extent of the rock riprap apron.

Spill-through Abutment

The observed vulnerable zone for incipient motion for this model was observed downstream of the contraction near the toe of the abutment (figure 7). The acceleration of flow through the slope of the spill face of the abutment parallel to the flow and the turbulence developed at the most contracted section of a stream jet are believed to have influenced the gravel failure at the mentioned zone. With the flow depth and velocity measured at the approach and for a computed discharge at the approach representing the design discharge, the velocity and flow depth were also computed at the contracted zone in the flood plain using equations (11) and (12). Using equation (2), the sediment number, N_{sc} , was computed with V_{cc} . The values of N_{sc} were plotted versus the D_{50}/d_{cc} ratio. Figure 11 shows a plot of the individual computed sediment numbers curve for the spill-through abutment for $D_{50} = 7.62$ mm (0.30 in) and 10.16 mm (0.40 in) for obstructed flow.

Because of the adverse slope obtained by regression analysis and the insufficient data at D_{50}/d_{cc} ratio smaller than 0.03, an average N_{sc} of 2.09 and 1.67 was taken for $D_{50} = 7.62$ mm (0.30 in) and 10.16 mm (0.40 in), respectively. A combined sediment number curve was obtained by averaging all the computed N_{sc} values for the two gravel sizes used during the experiments (figure 12). As a result, the average value of N_{sc} was found to be 1.87.

Although the scatter of data on the vertical wall and spill-through experiments is similar, the effect of D_{50}/d_{cc} was found to be less significant for the spill-through abutment.

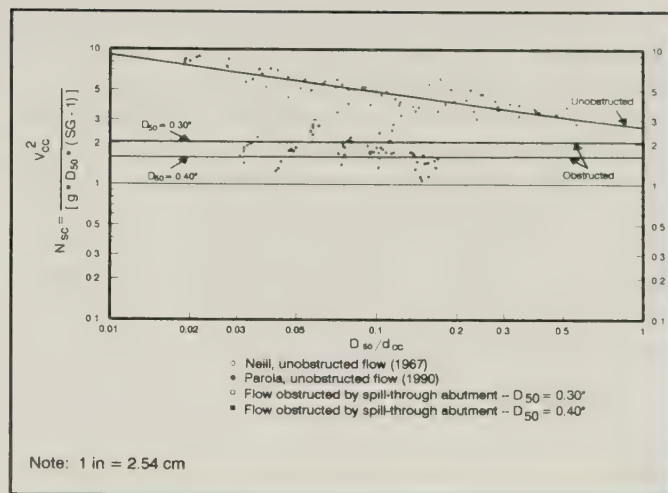


Figure 11.—Individual sediment number curve for spill-through abutment.

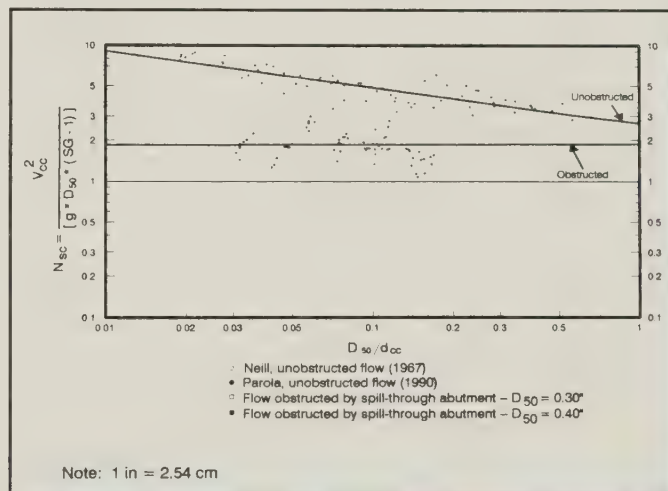


Figure 12.—Combined sediment number curve for spill-through abutment.

Figure 12 also indicates that for the spill-through model, depth is an important factor in determining the stability of the rock riprap when compared to the unobstructed flow curve. This figure also indicates that for the spill-through abutment, the velocity that caused the incipient motion of the gravel in the flood plain near the toe of the abutment should have been at least that for the unobstructed flow.

Therefore, to determine the stable size of rock riprap, equation (2) should be used as follows:

$$D_{50} = \left(\frac{0.535 * V_{cc}^2}{g * (SG - 1)} \right) \quad (16)$$

Figure 13 presents a plot of V_{cp} / V_{cc} versus X_t / W_{t-c} . The velocity ratio, V_{cp} / V_{cc} , and V_{cp} , X_t and W_{t-c} remain as previously defined. The plot shows that the effect of the abutment diminishes quickly with distance from the abutment.

At $X_t / W_{t-c} = 0$, and for 97 percent of the computations, the ratio of V_{cp} / V_{cc} fell near 2.0. At $X_t / W_{t-c} = 0$, and for 3 percent of the computations, the ratio of V_{cp} / V_{cc} reached 2.135.

The ratio of V_{cp}/V_{cc} also represents the indirect method—or “simple multiplier”—that should be applied to the averaged computed contracted velocity in the contraction within the flood plain to obtain the velocity near the abutment face that caused the incipient motion of the gravel.

The local effective velocity had no resemblance to what actually occurred around the abutment, but it was a convenient parameter to use in developing a simple multiplier ($V_{cp}/V_{cc} = 2.0$) for the velocity term in the rearranged Isbash equation (equation 3). Similarly to vertical-wall abutment, the velocity term within equation (3) can be multiplied by 2.0 to compute the rock riprap size for the spill-through abutment.

As with the other model, the discharge was also increased by 1.7 times the discharge that caused the incipient motion of the gravel to observe the extent of the failure zone. (8) This demonstrated that the rock riprap apron should be extended along the entire length of the abutment, both upstream and downstream, and to the parallel face of the abutment to the flow.

Figure 13 also illustrates that the velocity amplification decays rapidly with distance from the toe of the abutment and that the effect of the abutment occurs in a small portion of the contracted area. Therefore, as with the vertical-wall abutment, it would be reasonable to limit the rock riprap apron to a relative small portion of the constriction. Again, however, additional data analysis is needed to determine the extent of the rock riprap apron for this model.

Conclusions

The location for the most critical failure zone on an abutment encroaching the free flow of water on an armored flood plain depends on the abut-

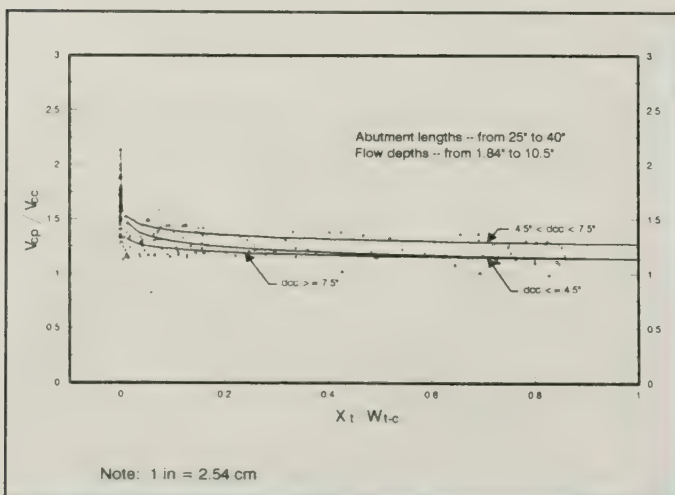


Figure 13.—Point velocity ratio for spill-through abutment.

ment shape. For the vertical-wall abutment model, the critical failure zone occurs at the upstream corner of the abutment and expands downstream towards the abutment and away from the toe with time and increase in discharge. For the spill-through abutment model, the critical failure zone is located downstream of the contraction near the toe and “grows” downstream and upstream of the constriction expanding to the toe and away from the abutment.

The turbulence of flow and vorticity generated near the face of the abutment are the causes of rock riprap failure. The velocities diminish in intensity and stabilize as distance from the toe of the abutment increases.

Equation (15) can be used to determine a stable rock riprap size to protect the toe of the vertical-wall abutment. Equation (16) can be used for spill-through abutment. (Note that use of these equations are limited to abutments encroachments up to 28 percent onto the flood plain for vertical-wall abutment shapes and 56 percent for spill-through abutment shapes—without counting the dimension of the main channel.)

The recommended rock riprap thickness should be equivalent to two times D_{50} . The average velocity in the flood plain within the constricted section should be used in equations (15) and (16).

The velocity multipliers found in this research for the vertical-wall and spill-through abutments, respectively, can be applied to the velocity term in the rearranged Isbash equation (equation 3) for sizing a stable rock riprap size for abutment protection.

Further data analysis is needed to determine the extension of the rock riprap apron for both vertical-wall and spill-through abutments.

Further research is needed to investigate the effect of:

- A greater encroachment onto the flood plain on the stability of the rock riprap.
- The abutments in a skew to the flow.
- The main channel in the stability of the rock riprap.

References

- (1) H.K. Liu, F.M. Chang, M.M. Skinner. “Effect of Bridge Constriction on Scour and Backwater,” Colorado State University, Fort Collins, CO, February 1961.
- (2) Jorge E. Pagán-Ortiz. “Stability of Rock Riprap for Protection at the Toe of Abutments Located at the Flood Plain.” Publication No. FHWA-RD-91-057, Federal Highway Administration, September 1991.

(3) Jorge E. Pagán-Ortiz. "Stability of Rock Riprap for Protection at the Toe of Abutments Located at the Flood Plain," masters thesis, The George Washington University, Washington, DC, December 1990.

(4) S.V. Isbash. "Construction of Dams by Depositing Rock in Running Water," *Communication No. 3*, Second Congress on Large Dams, Washington, DC, 1936.

(5) Arthur Parola, Jr. "The Stability of Riprap Used to Protect Bridge Piers," doctoral dissertation, State College, Pennsylvania State University, May 1990.

(6) Charles R. Neill and M. Selim Yalin. "Quantitative Definition of Beginning of Bed Movement," *Journal of the Hydraulics Division*, Proceedings of the American Society of Civil Engineers, Volume 95, No. HY1, January 1969.

(7) Scour Around Bridges, Research Report No. 13-B, Highway Research Board, Washington, DC, 1951.

(8) E.V. Richardson, Lawrence J. Harrison, and Stanley R. Davis. "Evaluating Scour at Bridges," *Hydraulic Engineering Circular No. 18*, Federal Highway Administration, Washington, DC, February 1991. List of figures

Jorge E. Pagán-Ortiz is a hydraulic engineer, Federal Highway Administration, Bridge Division, Hydraulics and Geotechnical Branch. He has presented FHWA guidelines and related microcomputer software in Latin America and is a member of the Pan American Institute of Highways. Mr. Pagán-Ortiz's received a masters degree in Civil Engineering with concentration in Water Resources Engineering. His thesis involved the determination of stability of rock riprap for the protection at the toe of abutments located in flood plains.

The FHWA Test Road: Construction and Instrumentation

by Kevin Black and William Kenis

Introduction

Three valuable resources give the Federal Highway Administration (FHWA) the capability to perform full-scale local tests on highway pavements. These resources are located at the Turner-Fairbank Highway Research Center (TFHRC) in McLean, Virginia:

- The **Pavement Test Facility**, which includes the fixed-speed rolling wheel Accelerated Loading Facility (ALF).^(1,2) This facility provides information on ultimate response (e.g., fatigue cracking and rutting) of flexible pavements in a matter of months; thus, problems and likely modes of failure can be identified long before they would occur on inservice highways.
- The **Pavement Isothermal Test System (PITS)**, which consists of two concrete chambers containing full-scale pavements. These pavements can be subjected to any configuration of controlled stress fixed-position loading in order to simulate a variety of highway load magnitudes and frequencies.
- The **Test Road Facility**, which is used to monitor the pavement's primary response when it is subjected to different types of moving axle suspension systems and truck configurations.

The FHWA is now constructing a fourth pavement test facility, a prototype dynamic truck actuation laboratory (DYNTRAC) to study the nature of dynamic forces on pavements induced by heavy trucks. DYNTRAC will measure the forces exerted by truck wheels as they are subjected to vertical oscillations simulating known road profiles.

Together, these facilities (see figure 1) will provide the basis for pavement research throughout the nineties. Studies at these laboratories, coordinated through the high priority research areas of Accelerated Evaluation of Pavement Performance and Truck-Pavement Interaction, will provide solutions to pavement infrastructure deterioration.

This article discusses the Test Road Facility constructed during the summer of 1990. The first test series, "Test Series I" was conducted in August of 1990. Data gathered from these tests were analyzed. Results to date are presented in

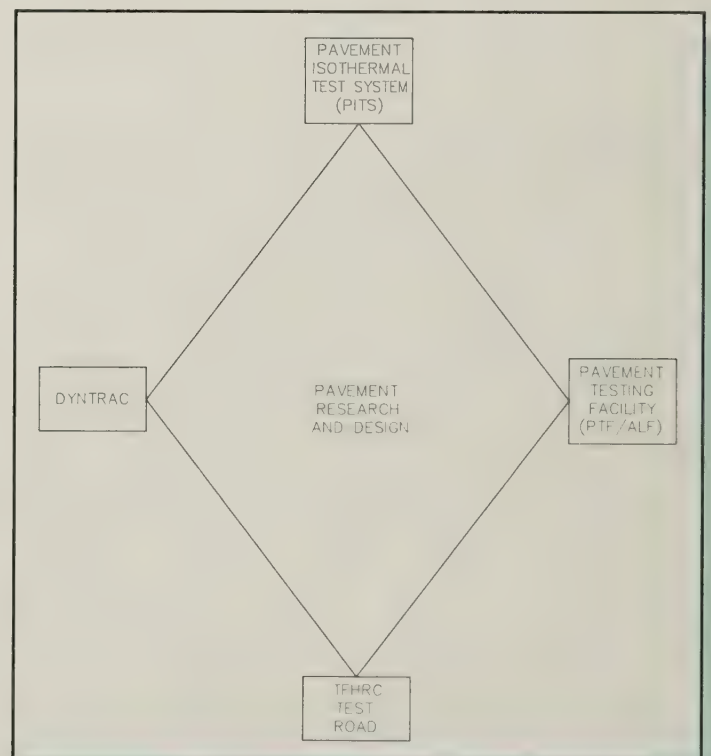


Figure 1.—Laboratories supporting pavement research.

¹Italic numbers in parentheses identify references on page 39.

three separate documents in terms of primary response load equivalency factors, primary deflection responses, and primary layer horizontal strain responses. (3,4,5)

Test Road Facility Overview

The Test Road Facility contains two full-scale flexible pavement test sections capable of accommodating any variety of vehicle types traveling at speeds up to 88 km/h (55 mi/h). The main feature of the Test Road is strain and deflection instrumentation—strategically located within the pavement sections—that measures primary responses to moving truck loads.

Experiments performed on the Test Road will study the effects of tire pressure and type, axle configuration and weight, suspension system type, truck configuration, and other truck traffic factors on pavement performance. Different combinations of these factors can cause greater or lesser wear to the highway pavement.

The data from the Test Road will be used to support the Truck-Pavement Interaction high priority area goals. These include:

- Verify layer theory and finite element primary response models.
- Develop primary response load equivalency factors, in terms of the standard 80,100 N (18-kip) axle, that express pavement damage attributed to vehicles with different weights and load distributions.
- Determine dynamic effects experienced by pavements as a result of the impact loading generated by the bouncing motion of vehicles induced by rough pavements.

Site Selection

Factors considered in choosing the Test Road site included safety, alignment, traffic volume, environmental impacts (such as noise), office and laboratory accessibility, and proximity to existing utilities. The site shown in figure 2 was selected because of its relatively straight alignment which permitted safer operation of trucks at maximum test speed.

A site investigation, which primarily entailed core drilling, was conducted to determine the *in situ* pavement conditions and estimate excavation quantities. Asphalt pavement thickness was found to be 165 mm (6.5 in); the base material was 381 mm (15 in) of bank-run gravel. The subgrade was a silty sand, classified as A-4, with a California bearing ratio (CBR) value of 5.

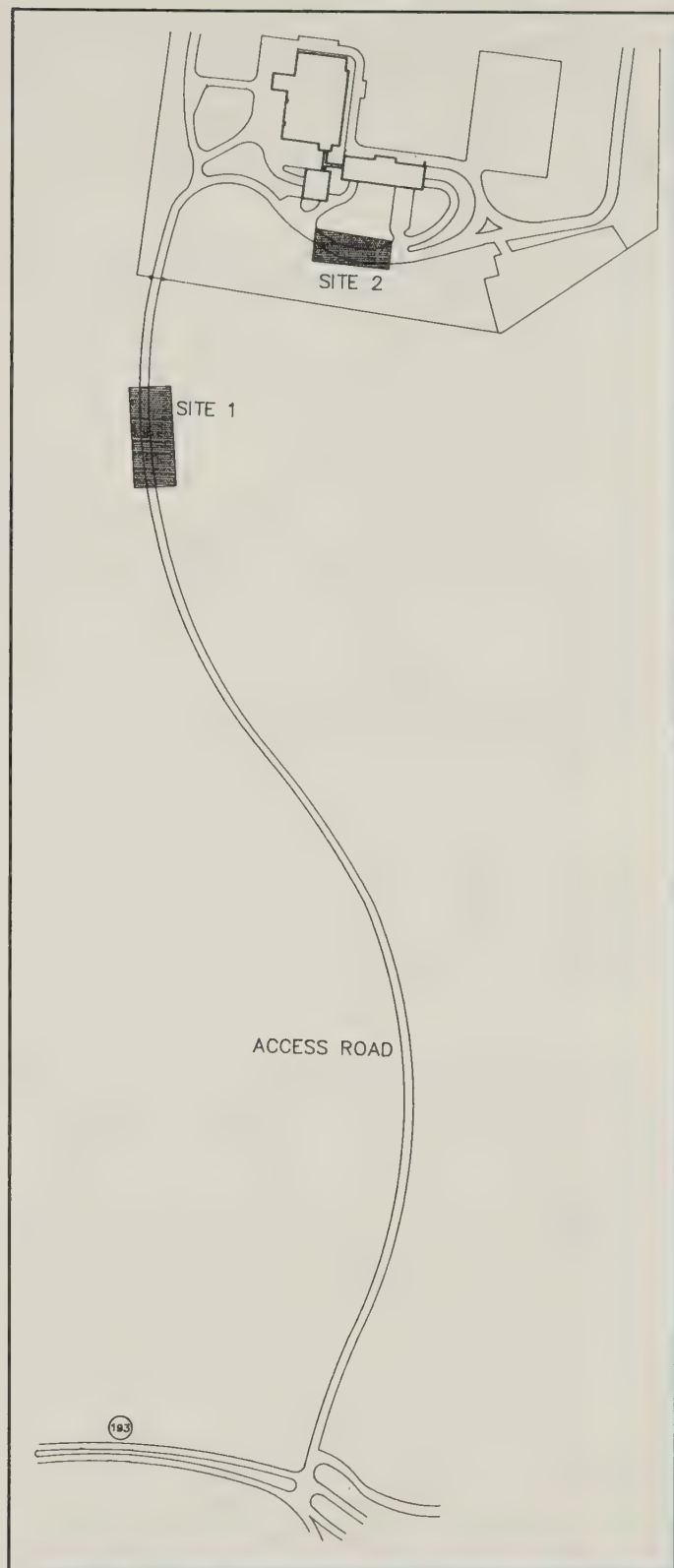


Figure 2.—Site identification at the TFHRC.

Design

The Test Road design only required reconstruction of the inbound lane of the access road connecting Virginia Route 193 with the TFHRC. The Test Road was designed to contain two 30-m (100-ft) test sections separated by a 7.6-m (25-ft) transition zone shown in figure 3. The thick pavement

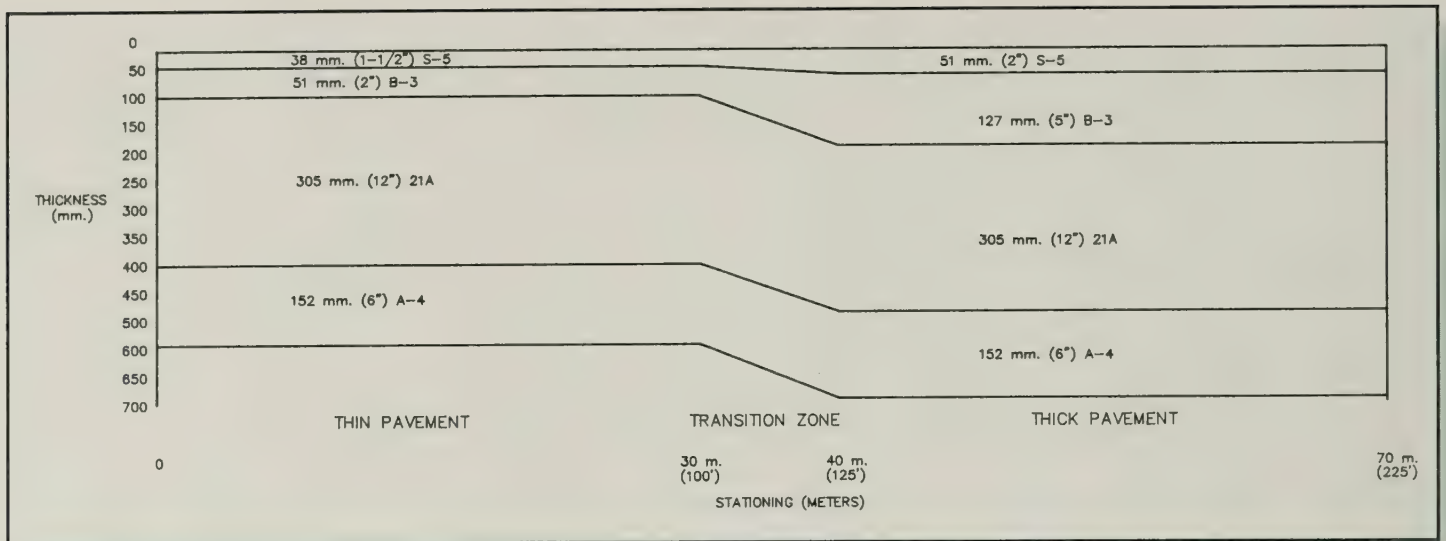


Figure 3.—Longitudinal cross section of thick and thin pavements at Test Road.

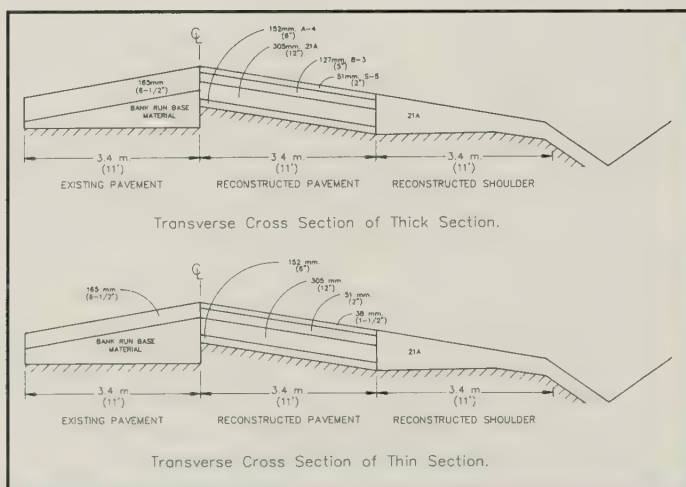


Figure 4.—Transverse cross section of thick and thin pavements at Test Road.

test section consisted of an A-4 subgrade overlaid with 152 mm (6 in) of A-4 subbase, a 305-mm (12-in) crushed stone base course, and topped with 178 mm (7 in) of asphalt concrete pavement. The thin section consisted of the same A-4 subgrade and 152 mm (6 in) of A-4 subbase overlaid by 305 mm (12 in) of crushed stone and a 89 mm (3.5-in) asphalt concrete pavement. A crushed stone shoulder 3.5 m (11 ft) wide and up to 0.6 m (2 ft) thick was added along the Test Road to serve as a working platform. Figures 3 and 4 illustrate the longitudinal and transverse cross sections of the road respectively. It is important to note that the Test Road thickness design is identical to the ALF Phase II thickness design. Construction materials included recycled asphalt concrete mix and dense graded crusher run limestone. The recycled asphalt concrete was a blend comprising about 85 percent virgin material. Lime was added to the asphalt concrete mix in accordance with Virginia Department of Transportation specifications, to reduce stripping (6).

The test sections were designed to accommodate strain and deflection instruments placed along the center of the left wheel path of each section; the transition zone was designed as a utility junction for the wires.

Construction

To construct the Test Road the old asphalt surface and bank-run gravel base had to be removed, and an additional 152 mm (6 in) of subgrade excavated, to eliminate any possible contamination of the subgrade and base course. This work entailed sawcutting 76.2 m (250 ft) of pavement and removing 152.9 m³ (200 yd³) of old material in preparation for placing the new pavement. Additional A-4 material was used to replace the mixed soil and bank-run base. This material was then rolled to seal it against water intrusion when placing the soil moisture gauges.

The crushed stone base was placed in 152-mm (6-in) lifts to a depth of 305 mm (12 in) and compacted to 2 290.9 kg/m³ (143 pcf). Construction then stopped for about a week as the strain gauges and parts of the single-point deflectometers were installed.

Next, a trenching machine was used to cut trenches to a instrumentation depth of about 0.6 m (2 ft) along the shoulder-pavement interface; these trenches were for collecting the wires in groups from feeder trenches.

One of the challenges of installing the instruments was ensuring that they were not damaged by the heat or vibration generated by paving and that the leads were buried to protect them from damage. Thirty-three H type strain gauges had their leads buried about 0.05 m (2 in) into the crushed stone base. This design was considered safe, but was

labor-intensive and could potentially disturb the integrity of the compacted stone base. In an effort to find an easier way to install the instrument leads without disturbing the previously compacted stone-base material, the leads of three other H-type gauges were wrapped in silicon-impregnated fiberglass tubing to prevent punctures from stones and to insulate the leads from the heat. The leads were then placed on top of the compacted base material where, for additional protection, they were covered with hand-placed hot mix asphalt about 1 hour before paving. Since these gauges functioned normally after paving, this method seemed to be effective. While the instruments were being placed, utility work was undertaken to provide electricity to the site.

Paving was done with a rubber-tired paver capable of straddling the instruments. The sawcut edges of the existing pavement were tack coated with an emulsion, as was the priming of the crushed aggregate base, to form a seal and bond the new surface to the existing pavement. Surface mix material was hand placed to cover some of the gauges. Paving progressed from the thick to the thin section, and was placed in 76-, 51-, or 38-mm (3-, 2-, or 1.5-in) lifts as appropriate. The paver's vibrating screed was used to develop a compaction density of 2 579.2 kg/m³ (168 pcf). The construction did not damage the instrumentation that had been installed.

Instrumentation

The Test Road's experimental sections were designed to collect primary response measurements (deflection, strain) and environmental data (moisture, temperature). These parameters are typically needed to verify the use of mechanistic models in pavement design and life-cycle analysis. The baseline pavement profile was

measured at completion of each layer to determine the variability of construction operation and provide initial elevation measurements for layer theory analysis. Table 1 shows the gauges installed, the parameters they measure, and the experiments in which they are used.

Pavement response is measured with strain gauges and deflectometers. The gauges installed were either the H-type (Kyowa) or a variety made by the Alberta Research Council (ARC). The deflectometers consisted of both single-layer and multilayer types and were installed in each section. The locations of the various instruments are shown in figure 5. A graphic display of each gauge is given in figure 6 a through f.

The **H-type gauges** were installed to measure the dynamic loading of the thick pavement section. To ensure their adherence to the underside of the asphalt pavement while retaining alignment along the path, the gauges were modified at the TFHRC Highway Electronics Laboratory. They were installed in a line of 36 gauges set 0.305 m (1 ft) apart.

The **ARC strain gauges** were placed to study strain in the pavement under controlled loading conditions. These gauges were placed in a pattern to cover the vehicle wheel print. A configuration of two rows of two in each section was used for redundancy.

Deflectometers were installed to evaluate the degree to which the pavement layers deflect. The single-layer or single-point deflectometers, also supplied by ARC, were used in coordination with the ARC strain gauges. Multidepth deflectometers were used to evaluate the compressive strains occurring in the lower structural layers. These instruments were fabricated at Texas A&M Univer-

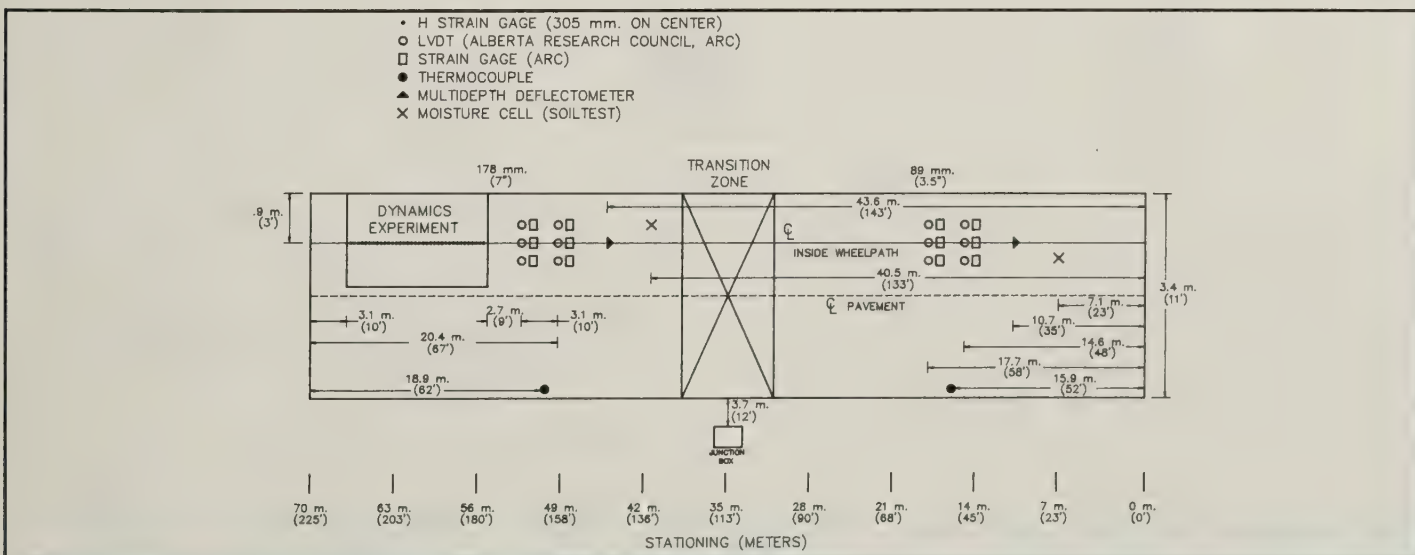


Figure 5.—Location of instruments in pavement sections.

sity. Both types of deflectometers are linear variable differential transformers; they were anchored at a depth of about 3 m (10 ft) to isolate them from vibration, noise, and settlement.

Table 1.—Summary of instruments and functions

Instrument	Measured property	Experiment
"H" strain gauge	Strain	Dynamics
ARC strain gauge	Strain	Response
Single layer deflectometer	Deflection	Response
Multilayer deflectometer	Deflection	Response
Moisture cell Environment	Moisture content	
Thermocouple Environment	Temperature	

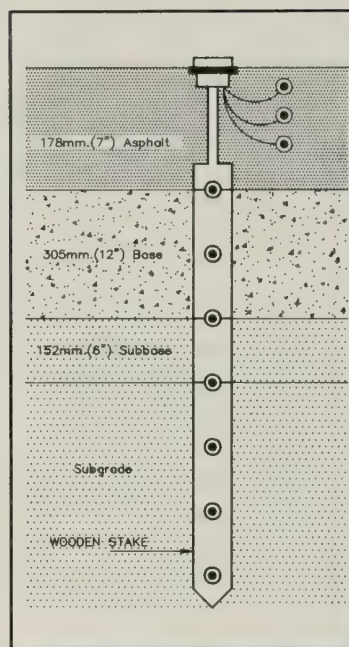


Figure 6a.—Thermocouple.

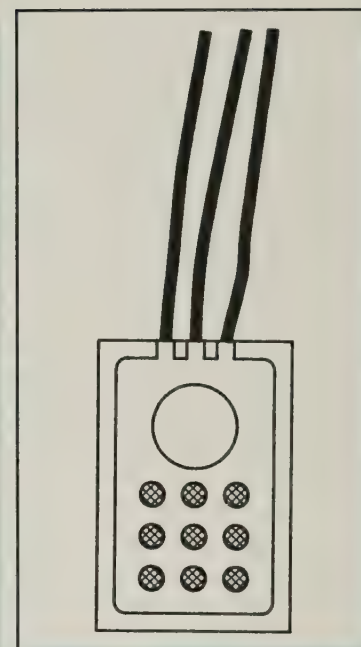


Figure 6b.—Moisture cell.

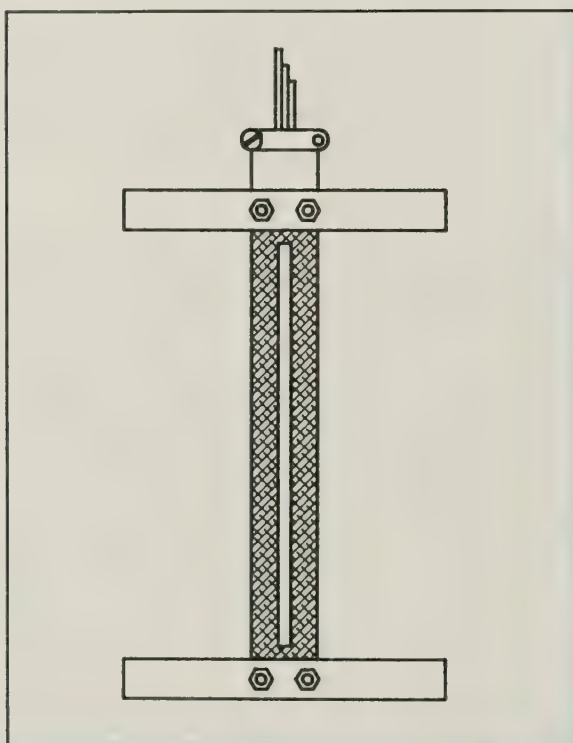


Figure 6c.—FHWA H strain gauge.

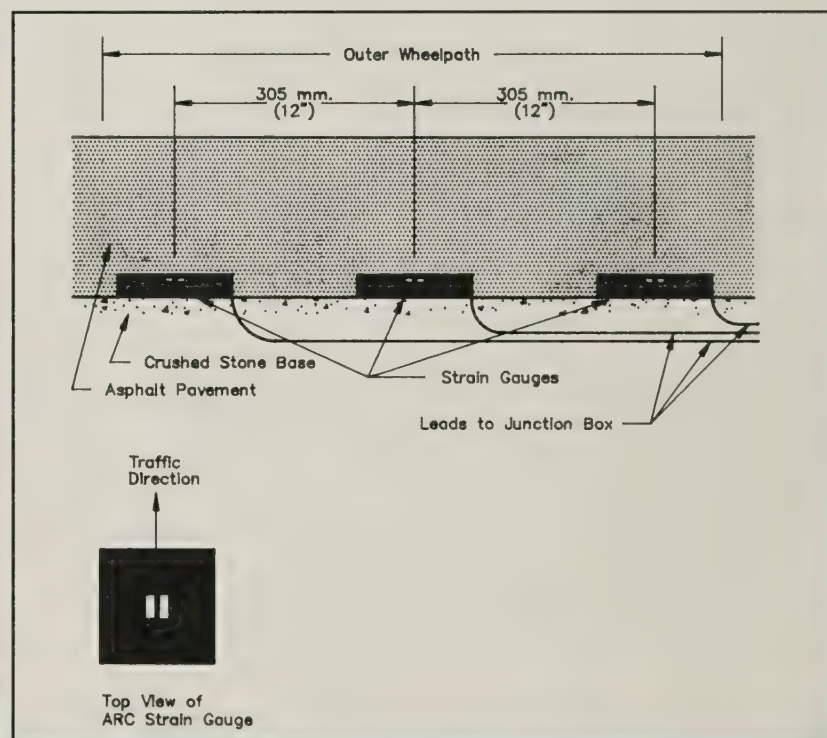


Figure 6d.—ARC strain gauge.

The **environmental gauges** were used to correlate the weather and climatic conditions to the responses measured. Soil moisture was measured using gauges placed 152 mm (6 in) and 305 mm (12 in) into the subgrade under each section.

Thermocouples were installed to measure the temperature changes in the pavement during testing. Each section contained one set of in-

struments; these provide temperature information at seven locations from the pavement surface to a depth of 1.3 m (4 ft).

Truck-Pavement Interaction

The Test Road was developed to support the overall goals of the FHWA's high priority area on Truck-Pavement Interaction. The three phases are summarized:

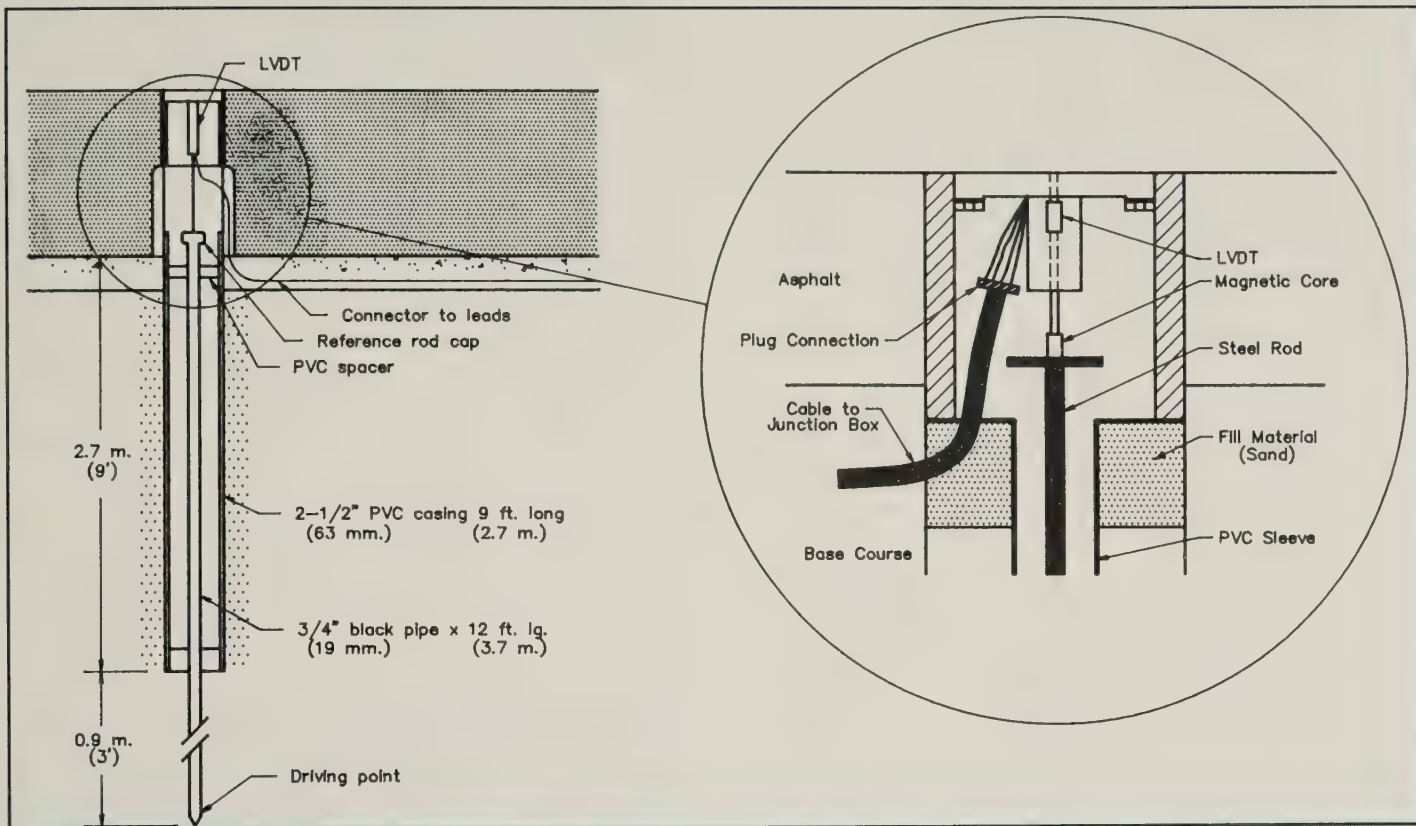


Figure 6e.—Single-layer deflectometer.

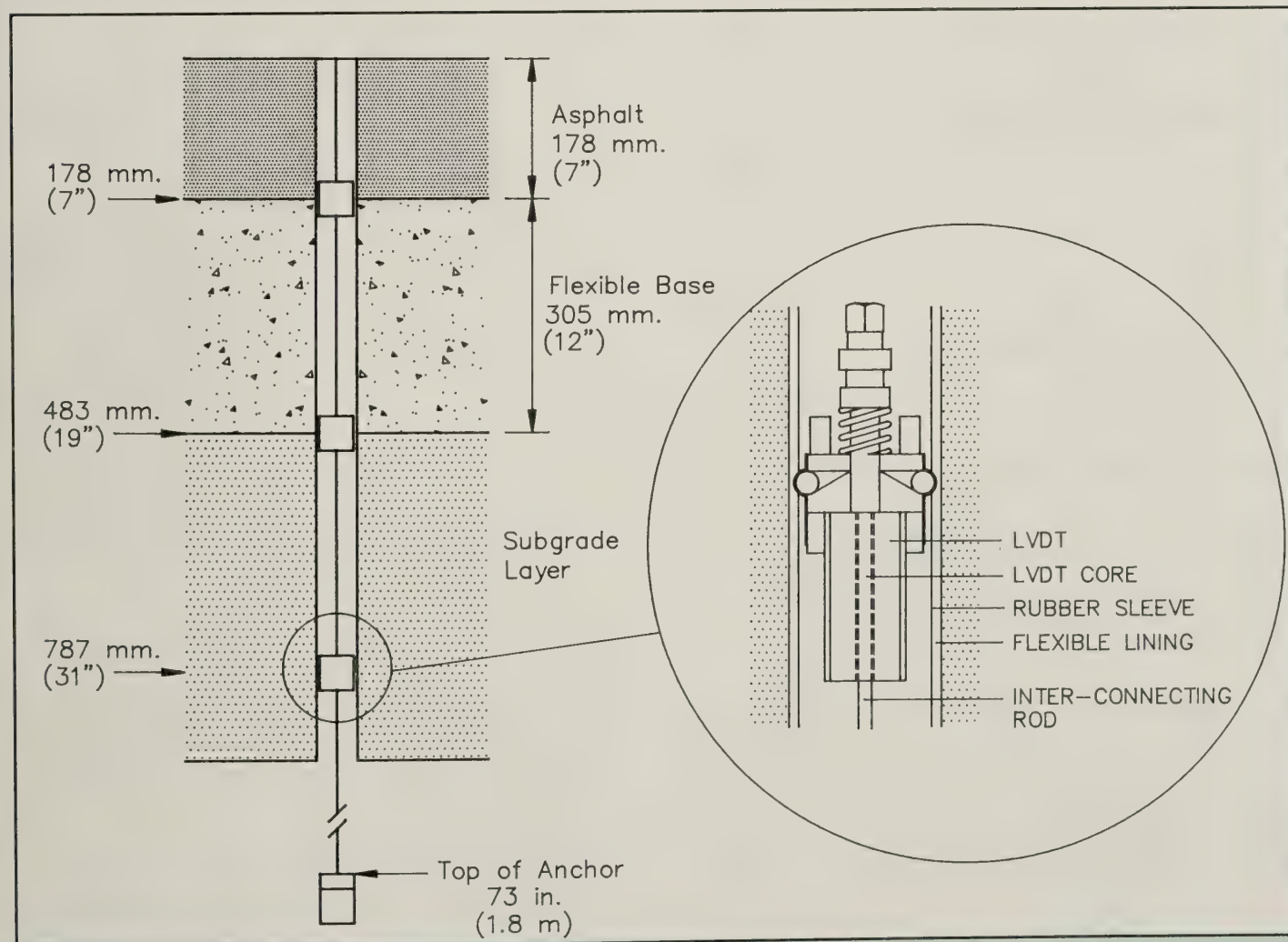


Figure 6f.—Multilayer deflectometer.

- Load Equivalency Factors (LEF's).
- Primary Response Analysis.
- Vehicle/Pavement Interaction.

Accomplished work in each phase will depend on the results from test conducted on the Test Road, ALF, PITS, and DYNTRAC.

Phase I: Load Equivalency Factors

This phase is substantially complete. Work comprised the design and construction of the Test Road, the conduct of Test Series I, and an evaluation report on the concept of primary response load equivalency. (3)

Initial testing was conducted in August 1990 on the Test Road's two instrumented test sections. The factors and levels included in the experiment are shown in table 2. The three vehicle types and axle loads used in the testing are shown in table 3. The single unit two-axle vehicle was used to apply the standard 8 172-kg (18-kip) load. The measured pavement primary responses were used, along with several selected primary response LEF methods, to develop LEF's and evaluate the accuracy and reliability of alternative methods (3). Some significant conclusions were:

1. Load level was the most significant factor.
2. Pavement thickness was relatively insignificant.
3. Slower vehicle speeds showed higher damage potential.
4. At the low and medium levels of axle loads, tire pressure had very little effect.
5. Deflection-based LEF methods are reasonable.

Phase II: Primary Response Analysis

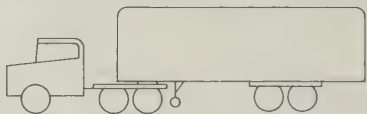
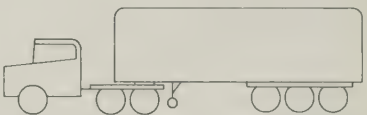
This phase of the research deals with the effects of load characteristics on the primary response of the pavement system and with the ability to estimate this occurrence using elastic and viscoelastic theory.

To determine the influence of vehicle parameters (load axle type, tire pressure) on pavement primary response, portions of the experimental data from Test Series I and II will be used. These responses will be analyzed in terms of the time-dependent and -independent plastic and viscoelastic properties of the pavement materials.

Table 2.—Factors and levels in experiment

Factors	Levels
Pavement structure—(PVMT)	weak, strong
Instruments nested in pavement—(INST)	4-sets (a duplicate set in each pavement)
Axle type	Single, tandem, tridem
Axle load	Low, Medium, High
Tire pressure	515-kPa (75-psi) 760-kPa (110-psi)
Speed	8-km/h (5-mi/h) 72-km/h (45-mi/h)

Table 3.—Vehicle classification and load distribution

TRUCK CLASSIFICATION	LOAD (KN)	TRUCK LOADS							
1	1 (HIGH) 2 (MEDIUM) 3 (LOW)								
		12.9					60.1		
		17.8					40.1		
		16.0					20.0		
2	1 (HIGH) 2 (MEDIUM) 3 (LOW)								
		18.7	48.1	47.7			49.0	48.1	
		18.7	36.1	36.1			31.2	38.3	
		18.7	22.3	22.3			20.0	24.5	
3	1 (HIGH) 2 (MEDIUM) 3 (LOW)								
		18.7	24.9	23.2			49.0	44.5	44.5
		18.7	21.4	20.5			33.4	31.2	31.2
		18.7	20.0	20.0			19.6	18.7	17.8

Phase III: Vehicle/Pavement Interaction

This effort will develop results from Test Series II at the Test Road, full-scale field tests at the ALF, laboratory tests using DYNTRAC, and computer simulations.

In Test Series II and field tests several types of trucks with different suspensions will be run on the Test Road. The trucks will be equipped with

wheel force transducers. Bumps will be placed on the pavement so that response data can be obtained from the 36 imbedded H strain gauges.

Results from tests conducted on the DYNTRAC system will emulate the FHWA Test Road profile; these will be compared with the responses from the tests conducted on the Test Road. Results from the ALF on dual versus single tires will be combined with predictors of flexible pavement testers to validate a new mechanistic submodel of VESYS.

Summary

Predicting pavement responses under surface loads is an important component of the mechanistic analysis of flexible pavements. These responses are a function of both the pavement structure and load characteristics. Factors such as tire pressure, axle load, axle configuration, vehicle speed, layer thickness, and time-dependent material properties influence the response. The TFHRC Test Road was constructed to evaluate these functions as they relate to pavement design. The experiments conducted at this facility promise to provide important insight that will improve existing knowledge of the interactive relationship between vehicle performance and pavement behavior.

References

- (1) David A. Anderson, Walter P. Kilareski, and Zahur Siddiqui. *Pavement Testing Facility: Design and Construction*, Publication No. FHWA-RD-88-059, Federal Highway Administration, Washington, DC, August 1988.
- (2) David A. Anderson, Peter Sebaaly, Nader Tabatabaee, Ramon Bonaquist, and Charles Churilla. *Pavement Testing Facility: Pavement Performance of the Initial Two Test Sections*, Publication No. FHWA-RD-88-060, Federal Highway Administration, Washington, DC, December 1988.
- (3) Stuart W. Hudson, Virgil L. Anderson, Paul Irick, and R. Frank Carmichael III. *Impact of Truck Characteristics on Pavement Truck Load Equivalency Factors*, Publication No. FHWA-RD-91-064, Federal Highway Administration, Washington, DC, March 1991.
- (4) W.J. Kenis and Gustav Rhode. "Primary Response Under Heavy Truck Traffic," paper presented at the Seventh International Conference on the Design of Asphalt Pavements, Cambridge, England, August 1992.
- (5) W.J. Kenis. "Flexible Pavement Strain Response Under Moving Truck Traffic," paper presented at the Engineering Foundation Conference: Vehicle Road Interaction II, Santa Barbara, CA, June 1992.
- (6) *Road and Bridge Specification*, Virginia Department of Transportation, Richmond, VA, January 1987.

Kevin Black is a highway engineer in the Materials Branch, Construction and Maintenance Division, of the Federal Highway Administration (FHWA). Formerly, he was with the Pavements Division in the Office of Research and Development.

William Kenis is Program Manager for FHWA's Truck/Pavement Interaction high priority area in the Pavements Division, Office of Research and Development.

The following are brief descriptions of selected publications recently published by the Federal Highway Administration, Office of Research and Development (R&D). The Office of Engineering and Highway Operations R&D includes the Structures Division, Pavements Division, Materials Division, and Long-Term Pavement Performance Division. The Office of Safety and Traffic Operations R&D includes the Intelligent Vehicle-Highway Systems Research Division, Design Concepts Research Division, and Information and Behavioral Systems Division. All publications are available from the National Technical Information Service (NTIS). In some cases, limited copies of publications are available from the R&D Report Center.

When ordering from the NTIS, include the PB number (or the publication number) and the publication title. Address requests to:

National Technical Information Service
5285 Port Royal Road
Springfield, Virginia 22161

Requests for items available from the R&D Report Center should be addressed to:

Federal Highway Administration
R&D Report Center, HRD-11
6300 Georgetown Pike
McLean, Virginia 22101-2296
Telephone: (703) 285-2144

Development of an Integrated Survey Vehicle for Measuring Pavement Surface Conditions at Highway Speed, Vol. I: Technical Report, Publication No. FHWA-RD-RD-90-011

by Pavements Division

The objective of this study was to develop an integrated survey vehicle for measuring pavement surface conditions at highway speeds. Requirements and operating characteristics were determined for such a system, a design prepared, and initial and operating costs were estimated.

This volume contains a review of the data and measurement needs for pavement condition surveys. The equipment available and under development are identified with emphasis on measurements at highway speeds. Three potential survey vehicle designs are presented. A

complete, detailed design for the vehicle and the test equipment was prepared and each subpart discussed.

This volume is the first in a series. The other volume is: FHWA-RD-90-012 Integrated Survey Vehicle—Technical Details.

This publication may only be purchased from the NTIS. (PB No. 92-147339/AS, Price code: A08)

Impact test of Shakespeare Luminaire Supports, Model as 35, Publication No. FHWA-RD-90-056

by Design Concepts Research Division

This report contains the results of crash tests performed on the Shakespeare Company, model AS 35 fiberglass pole with an aluminum anchor base. The luminaire supports were tested at speeds of 20 mi/h (8.9 m/s) and 60 mi/h (26.8 m/s) at the Federal Outdoor Impact Laboratory (FOIL) with the breakaway bogie vehicle. The device was previously tested, results are reported in FHWA-RD-88-257. The anchor base was modified with a groove to allow the device to break away with a lower stub height.

This publication may only be purchased from the NTIS. (PB No. 90-200056/AS, Price code: A03)

Impact test of Shakespeare Luminaire Supports, Model AH 35, Publication No. FHWA-RD-90-058

by Design Concepts Research Division

This report contains the results of crash tests performed on the Shakespeare Company, model AH 35 fiberglass pole with an aluminum anchor base. The luminaire supports were tested at speeds of 20 mi/h (8.9 m/s) and 60 mi/h (26.8 m/s). This device was tested at the Federal Outdoor Impact Laboratory (FOIL) with the breakaway bogie vehicle. This device was previously tested under the Luminaire Support Capability Test Program with the results reported in FHWA-RD-88-258. The anchor base was modified with a groove to allow the device to break away with a lower stub height.

This publication may only be purchased from the NTIS. (PB No. 90-205170/AS, Price code: A03)

Evaluation of New Nuclear Density Gauges on Asphalt Concrete, Publication No. FHWA-RD-90-092

by Materials Division

This report documents an evaluation of the state-of-the-art capabilities of nuclear density gauges to monitor the density of asphalt concrete. In particular, providing immediate information on compaction by the use of roller-mounted gauges and measuring the densities of thin layers were addressed. The study included three phases: literature search, laboratory tests, and field trials.

The laboratory and field trials were carried out using five commercially available static gauges, two commercially available roller-mounted gauges, and one prototype roller-mounted gauge previously developed for the FHWA. Full-depth measurements were taken at one field site and thin-lift measurements were taken at two sites. At a fourth site, the three roller gauges were mounted on a compacting roller and used during paving operations. At a fifth site, an attempt was made to correlate surface roughness and the speed of the roller-mounted gauges with density measurement accuracy. The density measurement data and the correlation of these data with core data are presented.

Under carefully controlled laboratory conditions, the accuracy and precision of all the gauges were well within manufacturers' specifications. When compensated for chemical composition, lift thickness, and density of the underlying material, the depth sensitivity and the thin-lift measurement capabilities of the gauges were impressive. In the field, however, the correlation of individual gauge density readings with core density measurements and with each other ranged from excellent to fair. The inability to precisely field calibrate the gauges prior to each use hampered their performance.

The data show that, within limitations, static nuclear gauges can be used for acceptance testing of thin lifts, but only when all parameters affecting the measurements are precisely known. The dynamic gauges can be effectively used to monitor relative density growth.

Limited copies of this publication are available from the R&D Report Center. Copies may also be purchased from the NTIS. (PB No. 92-158435/AS, price code: A07)

Service Life of Retroreflective Traffic Signs, Publication No. FHWA-RD-90-101

by Information and Behavioral Systems Division

The ability to predict coefficient of retroreflection (R_A) values for inservice traffic signs is critical for the Federal Highway Administration's (FHWA) Sign Management System (SMS). Within the SMS, tools for predicting inservice retroreflective performance of traffic signs and for determining the motorist's visual needs are required. The research which focuses on the motorist's needs in terms of traffic sign luminance, legibility distance, conspicuity, etc., is ongoing by others. The project reported on here evaluated the effects of climatological and geographic variables on sign sheeting deterioration.

A national data collection effort was undertaken. Data samples from 6,275 traffic signs were collected across the country. The data collected included; sheeting retroreflectivity, ground elevation, orientation to the sun, date of installation, sheeting type, etc. Mathematical equations were developed using the key deterioration variables to predict inservice coefficient of retroreflectivity (R_A) and legend to background contrast ratios. The main difficulty in modeling sheeting deterioration was the result of the variation in the coefficient of retroreflectivity for new sheeting.

Limited copies of this publication are available from the R&D Report Center. Copies may also be purchased from the NTIS. (PB No. 92-162163/AS, price code: A06)

Driver Visibility Under Wet Pavement Conditions: Size, Shape, and Spacing of Object Markers/Delineators, Publication No. FHWA-RD-91-016

by Information and Behavioral Systems Division

This study sought to reduce the risks of wet, nighttime driving by determining the minimum visibility required of roadway delineators. To isolate the contributions that discrete delineators have on guidance vision and drivers' reactions, test subjects were shown electronically digitized photographs of wet, nighttime roadways to which simulated delineation was added. The delineators' apparent size, shape, spacing, and contrast were calculated from models describing the visible effects of various rain conditions and roadway geometries. Subjects' scores were based on the minimum delin-

eator contrast required to correctly identify curve directions in various scenes. A disproportionate number of older drivers were tested because this group especially needs enhanced delineation under these adverse seeing conditions. Of the noncontrast delineator variables studied, only spacing provided a statistically significant difference for both right and left curve groups, with wider spacing requiring greater contrast for correct response. The delineator size effect was non-significant for both test groups. The evaluation of delineator shape produced the greatest inconsistency across test groups; delineator shape effects were significant for the left curve test group only.

Age group was statistically significant for only one of the test groups, but as expected, subjects age 65 and over generally required greater contrast for correct identification of curve direction. Likewise, for the effects of rainfall, the trend was in the expected direction, with heavier levels of rainfall requiring greater contrast for a correct response.

Copies may be purchased from the NTIS. (PB No. 92-163641/AS, price code: A04)

Basic Study to Improve Speed and Efficiency of Vehicle/Barrier Simulations, Vol. I: Final Report, Publication No. FHWA-RD-91-035; Basic Study to Improve Speed and Efficiency of Vehicle/Barrier Simulations, Vol. II: Appendixes, Publication No. FHWA-RD-91-036

by Design Concepts Research Division

The CRUNCH, GUARD and BARRIER VII programs as well as three versions of the NARD program were reviewed to identify modeling limitations and numerical procedures employed by each program. Other, commercially available, software was also reviewed. Based on the reviews, numerous recommendations were made to incorporate changes to the FHWA programs to increase their accuracy/efficiency.

A subset of the recommended improvements were implemented in three of the programs: GUARD 3.0, NARD 1.0 and PCNARD. This effort included development of a separate preprocessor program for GUARD and NARD. The modifications resulted in the attainment of various levels of success ranging from very little to a very significant increase in accuracy/efficiency, depending on the modification.

Other activities included a state-of-the-art review of soil/post interaction and development of general guidelines for the selection of integration

time-step size. Some of the FHWA vehicle impact simulation computer programs were modified to improve their accuracy and/or efficiency.

This publication may only be purchased from the NTIS. (Vol. I: PB No. 92-134667/AS, price code: A04); (Vol. II: PB No. 92-134675/AS, price code: A99)

Evaluation of Volatile Organic Compound (VOC) Compatible High Solids Coating Systems for Steel Bridges, Publication No. FHWA-RD-91-054

by Materials Division

A number of solvent-based and water-based coating systems formulated with low volatile-organic compound (VOC) were studied to determine the effect of solvent reduction and solids increase on their performance on steel bridges. All the systems contained VOC contents lower than 340 g/l. These systems included zinc richs, epoxy mastics, two CALTRANS and silicone rubber systems. High-VOC solvent-based systems were used as controls. Two accelerated laboratory weathering regimens, a cyclic salt-fog/freeze exposure and an ultraviolet/condensation exposure, were utilized as evaluation tools. Adhesion strengths and gloss retention properties of the coating systems before and after the tests were also measured. The performances of four low-VOC and high-VOC coating pairs were compared by the cyclic salt-fog/freeze exposure which provides much more rapid failure within a reasonable timeframe. More importantly, a composite test rating and rank for the corrosion resistance of the candidate coating systems in this study was made.

From this study, the newly developed low-VOC coating systems were found to perform as well or better than their high-VOC counterparts. The water-based inorganic zincs exhibited the best performance. The poorly performing systems were silicone rubber, epoxy mastics, and the two CALTRANS systems. Most of the coating systems lost some degree of adhesion after both exposures. A low-VOC acrylic aliphatic polyurethane was found to be the best topcoat for gloss retention. The preliminary outdoor weathering results after 15 months of marine exposure gave trends similar to the accelerated laboratory results.

Limited copies of this publication are available from the R&D Report Center. Copies may also be purchased from the NTIS. (PB No. 92-158419/AS, price code: A03)

The Costs of Highway Crashes, Publication No. FHWA-RD-91-055

by Information and Behavioral Systems Division

In 1988, an estimated 14.8 million motor vehicle crashes involved 47,000 deaths and almost 5,000,000 injuries. More than 4.8 million years of life and functioning were lost. Crash costs totaled \$334 billion. They included \$71 billion in out-of-pocket costs, \$46 billion in wages and household production, and \$217 billion in pain, suffering, and lost quality of life. Half of the out-of-pocket costs were property damage costs; the rest were medical, emergency services, workplace, travel delay, legal, and administrative costs. Employers paid 20 percent of the out-of-pocket and productivity costs. The general public paid 48 percent. People involved in crashes and their families paid the remainder and suffered the pain.

The comprehensive costs presented here are appropriate for use in benefit-cost analysis. The costs/police-reported crash are \$2,723,000/K-fatal

\$229,000/A-incapacitating injury, \$48,000/B-nonincapacitating injury, \$25,000/C-possible injury, \$4,500/O-property damage only (these crashes include injuries missed by the police), and \$4,300/unreported crash. The most costly kinds of crashes include motorcycle, pedestrian, pedalcycle, alcohol-involved, and heavy truck. Minor rural collectors, local rural streets, and urban arterials are the most dangerous/vehicle-mile of travel (vmt). Motorcycles have safety costs of \$2.14/vmt, buses \$.24/vmt, heavy trucks \$.19/vmt, light trucks \$.16/vmt, and cars \$.12/vmt. In nonfatal collisions involving only occupants, the most harmful events with highest cost/injury involve, in order: trees, overturns, other fixed objects, and utility poles.

Limited copies of this publication are available from the R&D Report Center. Copies may also be purchased from the NTIS. (PB No. 92-163625/AS, price code: A08)

The following are brief descriptions of selected items that have been completed recently by State and Federal highway units in cooperation with the Office of Safety and System Applications and the Office of Research and Development (R&D), Federal Highway Administration. Some items by others are included when they are of special interest to highway agencies. All publications are available from the National Technical Information Service (NTIS). In some cases, limited copies of publications are available from the R&D Report Center.

When ordering from the NTIS, include the PB number (or the publication number) and the publication title. Address requests to:

National Technical Information Service
5285 Port Royal Road
Springfield, Virginia 22161

Requests for items available from the R&D Report Center should be addressed to:

Federal Highway Administration
R&D Report Center, HRD-11
6300 Georgetown Pike
McLean, Virginia 22101-2296
Telephone: (703) 285-2144

Synthesis of Safety Research: Pedestrians, Publication No. FHWA-TS-90-034

by Office of Technology Applications

Pedestrian accidents account for 15 to 20 percent of all motor-vehicle fatalities in the U.S. and more than 100,000 people injured or killed each year. A considerable amount of research has been conducted over the past 25 years to better define the pedestrian safety problem and to develop and evaluate potential countermeasures.

This report synthesizes past research on pedestrian safety. The topics include characteristics of pedestrian accidents, conflict analyses and hazard formulas, pedestrian safety programs, and countermeasures related to engineering and education.

When selectively used, many of the engineering treatments can be effective in reducing pedestrian deaths and injuries. Engineering measures discussed in this report include pedestrian barriers, crosswalks, signs, signals, right-turn-on-red, innovative traffic control devices, refuge islands, provisions for handicapped pedestrians, bus stop location, school trip safety, overpasses, sidewalks, and others.

Also discussed in the report are pedestrian educational programs which have been found to reduce 20 to 30 percent of pedestrian accidents involving young children. Model traffic regulation and enforcement programs are also important.

This report is an update of Chapter 16 "Pedestrian Ways" which was published by the Federal Highway Administration in *Synthesis of Safety Research Related to Traffic Control and Roadway Elements, Vol: II*, December 1982.

Limited copies of this publication are available from the R&D Report Center. Copies may also be purchased from the NTIS. (PB No. 92-151992/AS, price code: A06)

Guidelines on the Use of Changeable Message Signs, Vol. I, Publication No. TS-90-043 and Guidelines on the Use of Changeable Message Signs, Vol. II: Executive Summary, Publication No. FHWA-TS-91-002

by Office of Technology Applications

This report is intended to provide guidance on selection of the appropriate type of Changeable Message Sign (CMS) display, the design and maintenance of CMS's to improve target value and motorist reception of messages, and pitfalls to be avoided. This report updates the 1986 FHWA publication *Manual on Real-Time Motorist Information Displays*. The guidelines and updated information are based on research results and on practices being employed by highway agencies in the United States, Canada and western Europe. CMS technology developments since 1984 are emphasized. Since the use of matrix-type CMS's, particularly light-emitting technologies, has increased in recent years, matrix CMS's have received additional attention in this report.

The report concentrates on design issues relative to CMS's with special emphasis on visual aspects, but does not establish specific criteria to determine whether to implement displays. The intent is to address display design issues for diverse systems ranging from highly versatile signing systems integrated with elaborate freeway corridor surveillance and control operations to low cost, less sophisticated surveillance and signing systems intended to alleviate a single specific problem.

Limited copies of this publication are available from the R&D Report Center. Copies may also be purchased from the NTIS. (Vol. I PB No. 92-150200/AS, price code: A12; Vol. II PB No. 92-152008/AS, price code: A04)

Static Testing of Deep Foundations, Publication No. FHWA-SA-91-042

by Office of Technology Applications

A static load test is conducted to measure the actual response of a pile under applied load. Load testing provides the best means of determining pile capacity, and if properly designed, implemented, and evaluated should pay for itself on most projects.

This manual provides guidelines concerning the planning, conduct, and interpretation of results of load tests performed on driven piles and drilled shafts. Axial compressive, axial tensile and lateral pile load tests are covered. The appendices contain a glossary of load testing terminology, guideline specifications, suggested load test procedures, load test reporting requirements, load test forms, and telltale details.

Limited copies of this publication are available from the R&D Report Center. Copies may also be purchased from the NTIS. (PB No. 92-176817, price code: A08)

The Cone Penetrometer Test, Publication No. FHWA-SA-91-043

by Office of Technology Applications

The cone penetrometer test consists of pushing a series of cylindrical rods with a cone at the base into the soil at a constant rate of 2 cm/sec. Continuous measurements of penetration resistance on the cone tip and friction on a friction sleeve are recorded during the penetration. The Piezo-cone records pore pressures in addition to point and friction resistance.

The continuous profiles obtained with the cone penetrometer test allow the user to visualize the stratigraphy, to evaluate the soil type, to estimate a large number of fundamental soil parameters, and to directly design shallow and deep foundations subjected to vertical loads.

Limited copies of this publication are available from the R&D Report Center. Copies may also be purchased from the NTIS. (PB No. 92-177120, price code: A08)

The Flat Dilatometer Test, Publication No. FHWA-SA-91-044

by Office of Technology Applications

A dilatometer test consists of pushing a flat blade located at the end of a series of rods. Once at the testing depth, a circular steel membrane located on one side of the blade is expanded horizontally into the soil. The pressure is recorded at three specific moments during the test. The blade is then advanced to the next testing depth.

The design applications of the dilatometer test includes: deep foundations under horizontal and vertical load, shallow foundations under vertical load, compaction control, and any other geotechnical problems which can make use of the soil parameters obtained from the dilatometer test.

Limited copies of this publication are available from the R&D Report Center. Copies may also be purchased from the NTIS. (PB No. 92-178524, price code: A08)

7th International Conference on Asphalt Pavements: Design, Construction, and Performance

The international conferences on asphalt pavements were first held in 1962 and have been held every 5 years since. Known colloquially as the "Ann Arbor" conferences, they have highlighted new developments in pavement design, material characteristics and rehabilitation design, emphasizing the importance of sound theory and practical methods to improve design practice and providing a framework for better and more economic asphalt pavements for highways, runways and industrial areas. The 7th conference, scheduled for August 16 through 20, 1992 in Nottingham, U.K., will continue this theme but within a broader scope, embracing construction aspects, to assist the profession in moving away from reliance on purely empirical methods of design towards a more scientifically based approach.

This conference is expected to be of major significance for all engineers involved in asphalt pavement technology since it is being held at a time when important developments in the use of end-product performance based specifications are taking place. The E.C. and the U.S. are committed to this approach and many other countries are following their lead. The use of performance based tests for both conventional and modified binders will be debated at the conference and in a special session featuring the U.S. Strategic Highway Research Program (SHRP) products.

The construction sessions will address topics including the effects of construction quality on pavement performance, partnerships among contractors and highway agencies, and warranties. The performance sessions will deal with improved pavement evaluation techniques, including non-destructive testing, pavement rehabilitation and case histories. One session is being devoted to implementation of research and new technologies.

The 1992 conference will feature a look back at the achievements during the period 1962-1992. Initiated in 1962 by the University of Michigan and the Asphalt Institute, the first six conferences have contributed substantially to the development of technology in the following areas:

- 1) Analytically-based design for new pavements and overlays.
- 2) Material testing and characterization.
- 3) Pavement evaluation.
- 4) Pavement management.

The Proceedings also contain extensive information on the distress characteristics of paving materials. The problem of fatigue cracking was

well-defined in the first conference. Contributions in subsequent conferences have added significantly to the body of knowledge, the concepts of which are now incorporated in analytically-based pavement design methods. Significant contributions have also been made on the problems of rutting and thermal cracking.

The field of pavement design and rehabilitation is not a static one. New challenges to the pavement engineer are continually arising since our pavements are expected to serve ever increasing traffic, both in terms of load magnitude and repetitions, while sources of high quality materials are being depleted in many areas of the world. Consequently, there is a continuing need to develop new techniques and materials to meet these increasing demands. A major barrier to progress is the slow implementation of new technology. Hence the need for designers, contractors and agencies to work more closely together in order to "pave the gap" between research and practice, to ensure high quality performance for all asphalt pavements. The 7th conference has been specifically designed to bring the various participants together in the pursuit of excellence in asphalt pavements.

The conference is sponsored by the International Society for Asphalt Pavements (ISAP) which was founded in 1987. It provides, not only the organizational framework for the International Conferences on Asphalt Pavements, but also assists with other conferences and workshops designed to promote excellence in asphalt pavement technology.

For more information please contact: Office of Technology Applications, Federal Highway Administration, Washington, DC.

The following new research studies reported by the FHWA's Office of Research and Development are sponsored in whole or in part with Federal highway funds. For further details on a particular study, please note the kind of study at the end of each description:

- FHWA Staff and Administrative Contract Research contact *Public Roads*.
- Highway Planning and Research (HP&R) contact the performing State highway or transportation department.
- National Cooperative Highway Research Program (NCHRP) contact the Program Director, NCHRP, Transportation Research Board, 2101 Constitution Avenue, NW, Washington, DC 20418.
- Strategic Highway Research Program (SHRP) contact the SHRP, 818 Connecticut Avenue, NW, 4th floor, Washington, DC 20006.

NCP Category A—Highway Safety

A.5: Design

Title: BCT and Turndown Guardrail End Accidents (NCP No. 2A5d0252)

Objective: Based upon existing State accident data bases, determine the frequency and severity of guardrail accidents. Conduct up to three crash tests at the FOIL involving guardrail terminals. Based upon the results of the survey and crashtests, define additional research needs and identify promising approaches.

Performing Organization: Turner-Fairbank Highway Research Center, McLean, VA

Expected Completion Date: December 1992

Estimated Cost: \$48,000 (FHWA Staff Research)

Title: Effects of Highway Standards on Safety (NCP Project 17-9)

Objective: The objective of this research is to access the safety effects of highway design standards and to synthesize the findings into documents that will provide guidance in addressing safety needs, given limited resources and other constraints. The research should be limited to geometric, cross-sectional, and roadside design elements for all roadway types and environments. The composition of traffic and seasonal and daily variations are considered important aspects of this research.

Performing Organization: Bellomo-McGee Inc.

Expected Completion Date: December 1993

Estimated Cost: \$200,000 (NCHRP)

NCP Category B—Traffic Operations

B.3: Motorist-Highway System Interactions

Title: Improved Traffic Control Device Design and Placement to Aid the Older Driver (NCP No. 5B3c0172)

Objective: Perform field oriented research investigation of older driver needs and capabilities as related to TCD design and implementation.

Performing Organization: Michigan State University, East Lansing MI 48824

Expected Completion Date: September 1994

Estimated Cost: \$350,000 (FHWA Administrative Contract)

NCP Category C—Pavements

C.2: Evaluation of Flexible Pavements

Title: A Comparison of Modified Open-Graded Friction Courses to Standard OGFC (NCP No. 4C2a2772)

Objective: Determine if improvements can be made to current GA open-graded friction courses by using modifiers including SBS, fibers, and crumb rubber. This is a laboratory and pavement study. The objective is to reduce oxidation and raveling.

Performing Organization: Georgia Department of Transportation, Atlanta, GA 30334

Expected Completion Date: September 1995

Estimated Cost: \$50,000 (HP&R)

NCP Category D—Structures

D.1: Bridge Design

Title: Nondestructive/destructive Tests and Associated Studies on Two Decommissioned Steel Truss Bridges (NCP No. 4D1a3522)

Objective: The objectives of this study are: To generate an experimental knowledge base regarding the actual capacity and failure mode of older steel truss bridges; to utilize the observed failure limit state behavior of two test bridges; and to extend the nondestructive bridge diagnostics and strength evaluation procedure which has been developed by university researchers to aged and deteriorated steel truss bridges. The study will focus on two old steel truss bridges scheduled to be removed from service. The investigation will involve finite element modeling, nondestructive testing using static and moving truck loads, and destructive load testing using a hydraulic actuator system installed at each site.

Performing Organization: University of Cincinnati, Cincinnati OH 45221

Funding Agency: Ohio Department of Transportation

Expected Completion Date: August 1994

Estimated Cost: \$699,000 (HP&R)

NCP Category E—Materials and Operations

E.1: Asphalt and Asphaltic Mixtures

Title: European Asphalt-Aggregate Mixture Analysis System NCP No. (4E1d2080)

Objective: Improve the quality of flexible pavements by demonstrating a European asphalt-aggregate mixture analysis system.

Performing Organization: Colorado Department of Highways, Denver, CO 80222

Expected Completion Date: December 1996

Estimated Cost: \$1,471,000 (HP&R)

Superintendent of Documents **Subscriptions Order Form**

S3

Order Processing Code:

***5119**

Charge your order.
It's Easy!



To fax your orders (202) 512-2233

YES, enter my subscription(s) as follows:

The total cost of my order is \$_____. International customers please add 25%. Prices include regular domestic postage and handling and are subject to change.

(Company or Personal Name) (Please type or print)

(Additional address/attention line)

(Street address)

(City, State, ZIP Code)

(Daytime phone including area code)

(Purchase Order No.)

YES NO

May we make your name/address available to other mailers?

Please Choose Method of Payment:

Check Payable to the Superintendent of Documents

GPO Deposit Account -

VISA or MasterCard Account

(Credit card expiration date) **Thank you for your order!**

(Authorizing Signature)

Mail To: New Orders, Superintendent of Documents
P.O. Box 371954, Pittsburgh, PA 15250-7954

GPO Subject Bibliography

To get a complete free listing of publications and periodicals on highway construction, safety, and traffic, write to the Superintendent of Documents, Mail Stop : SSOP, Washington, D.C. 20402-9328, and ask for Subject Bibliography SB-03 Highway Construction, Safety, and Traffic.

US. Department
of Transportation

**Federal Highway
Administration**

400 Seventh St., S.W.
Washington, D.C. 20590

Official Business
Penalty for Private Use \$300

Second Class Mail
Postage and Fees Paid
Federal Highway Administration
ISSN No. 0033-3735
USPS No. 516-690

**in this
issue**

**Developing a Standard Approach
for Testing New Traffic Control
Signs**

**In-Vehicle Navigational Devices:
Effects on the Safety of Driver
Performance**

**Rock Riprap for Protection of
Bridge Abutments Located at the
Flood Plain**

**The FHWA Test Road:
Construction and Instrumentation**

Public Roads

A Journal of Highway Research and Development

DOT LIBRARY



00181255